Chemistry of *C*-Trimethylsilyl-Substituted Heterocarboranes. 25. Syntheses, Structures, and Reactivities of $GeCl_3$-Substituted Half-Sandwich Germacarboranes, *closo*-1-Ge-2-($SiMe_3$)-3-(R)-5-($GeCl_3$)-2,3-$C_2B_4H_3$ (R = $SiMe_3$, Me, and H)†

Narayan S. Hosmane,*,‡ Jimin Yang, Kai-Juan Lu, Hongming Zhang, Upali Siriwardane, M. Safiqul Islam, Julie L. C. Thomas, and John A. Maguire

Department of Chemistry, Southern Methodist University, Dallas, Texas 75275

Received March 13, 1998

Anhydrous $GeCl_4$ reacts with the *closo*-stannacarboranes 1-Sn-2-($SiMe_3$)-3-(R)-2,3-$C_2B_4H_4$ (R = $SiMe_3$ (**I**), Me (**II**), and H (**III**)) in the absence of solvents to give the corresponding *closo*-germacarboranes 1-Ge-2-($SiMe_3$)-3-(R)-5-($GeCl_3$)-2,3-$C_2B_4H_3$ (R = $SiMe_3$ (**IV**), Me (**V**), and H (**VI**)) in yields of 43%, 22%, and 51%, respectively. Despite the presence of two potential Lewis-acid sites, the reactions of the germacarboranes with the bases $C_{10}H_8N_2$, $C_8H_6N_4$, and $C_{15}H_{11}N_3$ produced exclusively 1-(L)-2-($SiMe_3$)-3-(R)-5-($GeCl_3$)-1,2,3-$GeC_2B_4H_3$ (L = $C_{10}H_8N_2$, R = $SiMe_3$ (**VII**) and Me (**VIII**); L = $C_{15}H_{11}N_3$, R = $SiMe_3$ (**XI**)) or, when L = $C_8H_6N_4$, the bridged complexes 1,1′-(2,2′-$C_8H_6N_4$)-[1-Ge-2-($SiMe_3$)-3-(R)-5-($GeCl_3$)-2,3-$C_2B_4H_3$]$_2$ (R = $SiMe_3$ (**IX**), Me (**X**)). The reaction of **IV** with (η^5-C_5H_5)Fe(η^5-$C_5H_4CH_2(Me)_2N$) produced a 1:1 mixture of the salt {[(η^5-C_5H_5)Fe(η^5-$C_5H_4CH_2$]$_2$N(Me)$_2$}$^+${$GeCl_3$}$^-$ (**XII**) and 1-Ge[(η^5-C_5H_5)Fe(η^5-$C_5H_4CH_2(Me)_2N$)]-2,3-($SiMe_3$)$_2$-5-(NMe_2)-2,3-$C_2B_4H_3$ (**XIII**), a germacarborane in which a NMe_2 group replaced the $GeCl_3$ moiety on the carborane cage. All compounds were characterized by their infrared and ^{1}H, ^{11}B, and ^{13}C NMR spectra, as well as chemical analysis. In addition, **IV**−**VII**, **IX**, and **XII** were characterized by single-crystal X-ray diffraction. The structures showed **IV**−**VI** to be half-sandwich complexes in which a Ge(II) was symmetrically bound to the C_2B_3 faces of the carboranes, with a Ge(IV) terminally bonded to the unique borons of the cages in a $GeCl_3$ group. The structures of the Lewis-base adducts, **VII** and **IX**, showed that the nitrogens of the bases were symmetrically bonded to the Ge(II) atoms. Coordination by the bases resulted in a slip distortion of the capping metal atoms toward the boron side of the cages. Compounds **XII** and **XIII** are the final products of a sequence of reactions, one of which involves the displacement of a [$GeCl_3$]$^-$ unit from the unique boron by a (η^5-C_5H_5)Fe(η^5-$C_5H_4CH_2(Me)_2N$) base, producing an intermediate that reacts further with another molecule of the base to give both **XII** and **XIII**. In no case was there any evidence of the Ge(IV) acting as a reactive Lewis-acid center. Ab initio molecular orbital calculations were used in rationalizing some of the synthetic and spectroscopic results obtained in this study.

Introduction

Research in the area of the main-group heterocarboranes in the MC_2B_4 cage system has been quite active in recent years, especially when M is a group 14 element.[1−6] All elements in that group have been inserted into carborane cages, and a wealth of structural information is available on a number of half-sandwich, *closo*-carboranes of germanium,[7,8] tin,[9,10] and lead,[11] as well as the full-sandwich, *commo*-complexes of silicon,[12]

† Dedicated with best wishes to Prof. Robert R. Holmes (University of Massachusetts) on the occasion of his 70th birthday.

‡ Camille and Henry Dreyfus Scholar.

(1) Todd, L. J. In *Comprehensive Organometallic Chemistry II*; Abel, E. W.; Stone, F. G. A.; Wilkinson, G., Eds.; Elsevier Science: New York, 1995; Vol. 1, Chapter 7, p 257.

(2) Hosmane, N. S.; Maguire, J. A. *Adv. Organomet. Chem.* **1990**, *30*, 99.

(3) Saxena, A. K.; Maguire, J. A.; Banewicz, J. J.; Hosmane, N. S. *Main Group Chem. News* **1993**, *1* (2), 14.

(4) Hosmane, N. S.; Maguire, J. A. *J. Cluster Sci.* **1993**, *4*, 297.

(5) Hosmane, N. S.; Maguire, J. A. In *Electron Deficient Boron and Carbon Clusters*; Olah, G. A., Wade, K., Williams, R. E., Eds.; Wiley: New York, 1991; Chapter 9, p 215.

(6) Saxena, A. K.; Maguire, J. A.; Hosmane, N. S. *Chem. Rev.* **1997**, *97*, 2421.

(7) Hosmane, N. S.; Islam, M. S.; Pinkston, B. S.; Siriwardane, U.; Banewicz, J. J.; Maguire, J. A. *Organometallics* **1988**, *7*, 2340.

(8) Siriwardane, U.; Islam, M. S.; Maguire, J. A.; Hosmane, N. S. *Organometallics* **1988**, *7*, 1893.

(9) (a) Hosmane, N. S.; de Meester, P.; Siriwardane, U.; Islam, M. S.; Chu, S. S. C. *J. Am. Chem. Soc.* **1986**, *108*, 6050. (b) Cowley, A. H.; Galow, P.; Hosmane, N. S.; Jutzi, P.; Norman, N. C. *J. Chem. Soc., Chem. Commun.* **1984**, 1564. (c) Hosmane, N. S.; de Meester, P.; Maldar, N. N.; Potts, S. B.; Chu, S. S. C. *Organometallics* **1986**, *5*, 772. (d) Hosmane, N. S.; Barreto, R. D.; Tolle, M. A.; Alexander, J. J.; Quintana, W.; Siriwardane, U.; Shore, S. G.; Williams, R. E. *Inorg. Chem.* **1990**, *29*, 2698.

(10) Hosmane, N. S.; Jia, L.; Zhang, H.; Maguire, J. A. *Organometallics* **1994**, *13*, 1411.

S0276-7333(98)00183-6 CCC: $15.00
Publication on Web 05/30/1998

germanium,[9a] and tin.[13] These studies show that a definite structure−oxidation state relationship exists in these systems; in the *closo*-complexes, the capping group 14 elements are in formal +2 oxidation states, while the *commo*-complexes contain these elements in their +4 states. The coordination chemistry of *closo*-$M^{II}C_2B_4$ metallacarboranes has also been investigated, and the structures of the resulting donor−acceptor complexes involving Lewis bases such as 2,2′-bipyridine ($C_{10}H_8N_2$), 2,2′-bipyrimidine ($C_8H_6N_4$), (ferrocenylmethyl)-*N*,*N*-dimethylamine, [(η^5-C_5H_5)Fe(η^5-$C_5H_4CH_2(Me)_2N$)], and 2,2′:6′,2″-terpyridine ($C_{15}H_{11}N_3$) have been reported.[14−16] The structures of these adducts show that despite having a "lone pair" of electrons, the capping M(II) element acts as the Lewis-acid site and bonds to the base. Coordination by the base leads to a distortion of the MC_2B_4 cage in that the metal atom is dislocated, or slipped, toward the boron side of the C_2B_3 face of the carborane ligand, which is normally the side over which the base resides. Similar Lewis-acid behavior and attendant distortions were found in the larger cage, *closo*-MC_2B_9 metallacarboranes.[9b,17] The Lewis acid−base behavior of the *commo*-M(IV) complexes is not straightforward. Hawthorne and co-workers studied the reaction of *commo*-3,3′-Si(3,1,2-$SiC_2B_9H_{11})_2$ with several Lewis bases.[18] They found that the reaction of the silacarborane with C_5H_5N produced a $(C_5H_5N)_2$Si-$(C_2B_9H_{11})_2$ complex in which a $(C_5H_5N)_2$Si group was exopolyhedrally bound to one of the carborane cages and endopolyhedrally bound to the other. On the other hand, the reaction of the silacarborane with Me_3P resulted in an attack on one of the cage borons rather than at the silicon atom.[18] These results raise the general question as to what would be the outcome of the reactions between Lewis bases and metallacarboranes possessing two potential metal acid sites, one in a +2 state and another in a +4 state. Our success in synthesizing the germacarborane, *closo*-1-Ge^{II}-2,3-$(SiMe_3)_2$-5-($Ge^{IV}Cl_3$)-2,3-$C_2B_4H_3$,[8] offers the opportunity to study such a system. In an effort to ascertain which germanium atom would be the preferred acid site and to obtain more information regarding the structure, bonding, and reactivity patterns of this new class of germacarboranes, a number of such species were synthesized and their reactivities explored. Here, we report the results of this study.

Experimental Section

Materials. The *closo*-stannacarborane precursors 1-Sn-2-($SiMe_3$)-3-(R)-2,3-$C_2B_4H_4$ (R = $SiMe_3$ (**I**), Me (**II**), and H (**III**)) were prepared using literature methods.[19] Before use, 2,2′-bipyridine (Aldrich), 2,2′-bipyrimidine (Lancaster Syntheses), 2,2′:6′,2"-terpyridine (Aldrich), and ferrocenylmethyl-*N*,*N*-dimethylamine (Strem Chemicals) were sublimed or distilled in vacuo and their purity was checked by IR and NMR spectroscopy and by melting point or boiling point measurements. Anhydrous $GeCl_4$ (Strem Chemicals) was passed through −78 °C traps in vacuo to remove any last traces of HCl impurity. Benzene, THF, *n*-hexane, and *n*-pentane were dried over $LiAlH_4$ and doubly distilled; all other solvents were dried over 4−8 mesh molecular sieves (Aldrich) and either saturated with dry argon or degassed before use.

Spectroscopic and Analytical Procedures. Proton, boron-11, and carbon-13 pulse Fourier transform NMR spectra at 200, 64.2, and 50.3 MHz, respectively, were recorded on an IBM-WP200 SY multinuclear NMR spectrometer. Infrared spectra were recorded on a Perkin-Elmer model 1600 FT-IR spectrophotometer and Nicolet Magna 550 FT-IR spectrophotometer. Elemental analyses were obtained from E+R Microanalytical Laboratory, Inc., Corona, NY.

Synthetic Procedures. All experiments were carried out in Pyrex glass round-bottom flasks of 250 mL capacity, containing magnetic stirring bars and fitted with high-vacuum Teflon valves. Nonvolatile substances were manipulated in either a drybox or evacuable glovebags under an atmosphere of dry nitrogen. All known compounds among the products were identified by comparing their IR and NMR spectra with those of authentic samples.

Synthesis of *closo*-1-Ge-2-($SiMe_3$)-3-(R)-5-($GeCl_3$)-2,3-$C_2B_4H_3$ (R = $SiMe_3$ (IV), Me (V), and H (VI)). Compounds **IV**, **V**, and **VI** were all synthesized from the reaction of $GeCl_4$ with 1-Sn-2-($SiMe_3$)-3-(R)-2,3-$C_2B_4H_4$ (R = $SiMe_3$ (**I**), Me (**II**), or H (**III**)) using the same reaction stoichiometries and experimental conditions. These conditions were determined from a careful product analysis study of the formation of **IV** (R = $SiMe_3$). Therefore, only this synthesis will be discussed in detail; the other syntheses were carried out similarly.

Anhydrous $GeCl_4$ (1.01 g, 4.71 mmol) was condensed into a 250-mL reaction flask containing the *closo*-stannacarborane 1-Sn-2,3-$(SiMe_3)_2$-2,3-$C_2B_4H_4$ (**I**) (1.51 g, 4.49 mmol) and a magnetic stirring bar. No solvent was condensed into the reaction flask. The resulting heterogeneous mixture was stirred constantly at 135−150 °C for 72 h, during which time the mixture turned dark brown in color. The reaction flask was cooled and then attached to a series of detachable U-traps, held at temperatures of 10, 0, and −196 °C. After complete removal of the volatile product and HCl (not measured), the dark brown residue in the reaction flask was heated to 135 °C in vacuo to collect a colorless crystalline solid, identified as *closo*-1-Ge-2,3-$(SiMe_3)_2$-5-($GeCl_3$)-2,3-$C_2B_4H_3$ (**IV**) (0.92 g, 1.96 mmol; 44% yield; mp 68 °C), in the detachable U-trap held at 0 °C. A substantial amount of the neutral *nido*-carborane precursor 2,3-$(SiMe_3)_2$-2,3-$C_2B_4H_6$ (0.22 g, 1.00 mmol) was collected in a vacuum-line trap held at −196 °C, while *commo*-1,1′-Ge-[2,3-$(SiMe_3)_2$-2,3-$C_2B_4H_4]_2$ (0.33 g, 0.65 mmol) was collected in a trap held at 10 °C. The sidearms of both the U-traps and reaction flask were wrapped with a heating tape to maintain a temperature range of 100−110 °C during sublimation. After complete sublimation, an off-white solid, identified as $SnCl_2$ (not measured), remained in the reaction flask and was discarded. In a like manner, 1-Sn-2-

(11) Hosmane, N. S.; Siriwardane, U.; Zhu, H.; Zhang, G.; Maguire, J. A. *Organometallics* **1989**, *8*, 566.
(12) (a) Hosmane, N. S.; de Meester, P.; Siriwardane, U.; Islam, M. S.; Chu, S. S. C. *J. Chem. Soc., Chem. Commun.* **1986**, 1421. (b) Siriwardane, U.; Islam, M. S.; West, T. A.; Hosmane, N. S.; Maguire, J. A.; Cowley, A. H. *J. Am. Chem. Soc.* **1987**, *109*, 4600.
(13) Jia, L.; Zhang, H.; Hosmane, N. S. *Organometallics* **1992**, *11*, 2957.
(14) (a) Hosmane, N. S.; Lu, K.-J.; Siriwardane, U.; Shet, M. S. *Organometallics* **1990**, *9*, 2798. (b) Hosmane, N. S.; Lu, K.-J.; Zhang, H.; Maguire, J. A.; Jia, L.; Barreto, R. D. *Organometallics* **1992**, *11*, 2458.
(15) (a) Hosmane, N. S.; de Meester, P.; Maldar, N. N.; Potts, S. B.; Chu, S. S. C.; Herber, R. H. *Organometallics* **1986**, *5*, 772. (b) Hosmane, N. S.; Islam, M. S.; Siriwardane, U.; Maguire, J. A.; Campana, C. F. *Organometallics* **1987**, *6*, 2447. (c) Hosmane, N. S.; Fagner, J. S.; Zhu, H.; Siriwardane, U.; Maguire, J. A.; Zhang, G.; Pinkston, B. S. *Organometallics* **1989**, *8*, 1769. (d) Siriwardane, U.; Maguire, J. A.; Banewicz, J. J.; Hosmane, N. S. *Organometallics* **1989**, *8*, 2792.
(16) (a) Hosmane, N. S.; Siriwardane, U.; Zhu, H.; Zhang, G.; Maguire, J. A. *Organometallics* **1989**, *8*, 566. (b) Hosmane, N. S.; Lu, K.-J.; Zhu, H.; Siriwardane, U.; Shet, M. S.; Maguire, J. A. *Organometallics* **1990**, *9*, 808.
(17) Jutzi, P.; Galow, P.; Abu-Orabi, S.; Arif, A. M.; Cowley, A. H.; Norman, N. C. *Organometallics* **1987**, *6*, 1024.
(18) Schubert, D. M.; Rees, W. S., Jr.; Knobler, C. B.; Hawthorne, M. F. *Organometallics* **1990**, *9*, 2938.
(19) Hosmane, N. S.; Sirmokadam, N. N.; Herber, R. H. *Organometallics* **1984**, *3*, 1665.

Table 1. FT-NMR Spectra Data[a] for *closo*-Germacarboranes and Their Donor−Acceptor Complexes (IV−XI) and Related Derivatives (XII−XIV)

compd	δ splitting, assignment ($^1J(^{11}B-^1H)$ or $^1J(^{13}C-^1H)$, Hz)	rel area
	200.13 MHz ^{1}H NMR Data[b]	
IV	3.79, q(br), basal H (133); 1.40, q(br), apical H (175); 0.46, s, $SiMe_3$	2:1:18
V	3.54, q(br), basal H (unresolved); 1.92, s, C−Me; 1.40, q(br), apical H (unresolved); −0.03, s, $SiMe_3$	2:3:1:9
VI	6.47, s(br), C−H; 4.25, q(br), basal H (unresolved); 1.19, q(br), apical H, (unresolved); −0.03, s, $SiMe_3$	1:2:1:9
VII	8.92, s, bipy ring; 7.41, d, bipy ring (unresolved); 7.21, t, bipy ring (6.23); 6.72, t, bipy ring (4.74), 5.40, q(br), overlapping, basal H (unresolved); 0.63, s, $SiMe_3$; 0.50, q(br), apical H (unresolved)	1:1:1:1:1:9:1
VIII	8.72, s, bipy ring; 7.41, d, bipy ring (unresolved); 7.06, t, bipy ring (unresolved); 6.88, t, bipy ring (unresolved); 4.90, q(br), overlapping, basal H (unresolved); 2.66, s, C−Me; 0.48, s, $SiMe_3$; 0.23, q(br), apical H (unresolved)	2:2:2:2:2:3:9:1
IX	8.51, d, bpmd ring (5.13); 6.45, t, bpmd ring (5.13); 5.20, q(br), basal H (unresolved); 0.30, s, $SiMe_3$; 0.41, q(br), apical H (unresolved)	2:1:1:18:1
X	8.41, d, bpmd ring (3.66); 6.38, t, bpmd ring (2.93); 4.97, q(br), basal H (unresolved); 2.43, s, C−Me; 0.30, s, $SiMe_3$; 0.20, q(br), apical H (unresolved)	4:2:2:3:9:1
XI	8.96, d, terpy ring; 8.26, d, terpy ring; 8.06, d, overlapping, terpy ring; 7.65, t, terpy ring; 7.04, t, terpy ring; 6.82, t, terpy ring; 5.26, q(br), basal H (unresolved); 0.21, s, $SiMe_3$; 0.50, q(br), apical H (unresolved)	2:2:2:1:2:2:2:18:1
XII	3.74, s, C_5H_4; 3.65, s, C_5H_5; 2.96, s, CH_2; 2.13, s, NMe_2	4:5:2:3
XIII	4.10, s(br), basal H (unresolved); 3.97, s, C_5H_4; 3.90, s, C_5H_5; 3.25, s, CH_2; 1.98, s, NMe_2; 1.76, s, B−NMe_2; 0.20, s, $SiMe_3$; 0.12, q(br), apical H (unresolved)	2:4:5:2:6:6:9:1
	64.21 MHz ^{11}B NMR Data[c]	
IV	23.59, br, basal B; −4.60, d, apical BH (146)	3:1
V	20.13, d, overlapping, basal BH (unresolved); −3.45, d, apical BH (174)	3:1
VI	21.89, d, basal BH (123); 19.25, s, basal B−Ge; −5.09, d, apical BH (174)	1:2:1
VII	20.86, d(br), basal BH (unresolved); 13.74, s(br), basal B−Ge; −28.05, d, apical BH (174)	1:2:1
VIII	11.45, d(br), basal BH (unresolved); −25.07, d(br), apical BH (unresolved)	3:1
IX	17.60, br, basal B; −23.98, d, apical BH (unresolved)	3:1
X	20.89, d(br), basal B (unresolved); −14.58, d, apical BH (unresolved)	3:1
XI	26.27, br, ill-defined peak, basal B; −10.38, d, apical BH (160)	3:1
XII	no boron present	
XIII	36.75, d(br), basal B (unresolved); 8.6−6.8, br, basal B; −11.78, d(br), apical BH (unresolved)	1:1:1:1
	50.32 MHz ^{13}C NMR Data[d]	
IV	133.65, s, cage C (SiCB); 1.10, q, $SiMe_3$ (120)	1:3
V	133.21, s, cage C (SiCB); 130.54, s(br), cage C (CCB); 22.17, q, C−Me (128); 0.11, q, $SiMe_3$ (120)	1:1:1:3
VI	132.15, s(br), cage C (SiCB); 118.18, d, cage CH (189); 0.79, q, $SiMe_3$ (120)	1:1:3
VII	149.57, s, bipy ring; 145.17, d, bipy ring (183); 139.37, d, bipy ring (165); 133.01, s, cage C (SiCB); 125.41, d, bipy ring(176); 121.65, d, bipy ring (165); 2.38, q, $SiMe_3$ (118)	1:1:1:1:1:1:3
VIII	149.35, s, bipy ring; 145.13, d, bipy ring (183); 139.84, d, bipy ring (168); 133.01, s, cage C (SiCB); 125.66, d, bipy ring (105); 121.99, d, bipy ring (170); 115.21, s, cage C (CCB); 22.87, q, C−Me (125); 1.23, q, $SiMe_3$ (120)	2:2:2:1:2:2:1:1:3
IX	161.74, s, bpmd ring; 157.52, d, bpmd ring (187); 135.02, s, cage C (SiCB); 121.05, d, bpmd ring (165); 2.13, q, $SiMe_3$ (116)	1:2:2:1:6
X	157.47, s, bpmd ring; 156.23, d, bpmd ring (186); 134.88, s, cage C (SiCB); 122.59, d, bpmd ring (170); 112.02, s, cage C (CCB); 21.98, q, C−Me (127); 1.14, q, $SiMe_3$ (118)	1:2:1:1:1:1:3
XI	148.67, s, terpy ring; 146.62, s, terpy ring; 145.01, d, terpy ring (130); 142.31, s, terpy ring; 136.42, d, terpy ring (156); 132.44, d, terpy ring (163); 123.75, d, terpy ring (154); 122.67, d, terpy ring (146); 119.40, s(br), cage C (SiCB); 1.61, s, $SiMe_3$ (120)	2:2:2:1:2:2:2:2:2:6
XII	72.12, s, ferrocenyl C; 69.89, d, C_5H_4 (176); 69.01, d, C_5H_5 (176); 47.41, t, CH_2 (144); 41.83, q, NMe_2 (140)	1:4:5:1:1
XIII	139.28, s, cage C (SiCB); 83.40, s, ferrocenyl C; 70.47, d, C_5H_4 (170); 69.62, d, C_5H_5 (176); 58.43, t, CH_2 (140); 43.70, q, NMe_2 (135); 39.35, q, B−NMe_2 (140); 1.79, q, $SiMe_3$ (118)	2:1:4:5:1:2:2:6

[a] C_6D_6 was used as the solvent and an internal standard of $\delta = 7.15$ ppm in the ^{1}H NMR spectra and $\delta = 128.0$ ppm in the ^{13}C NMR spectra with a positive sign indicating a downfield shift. Legend: s = singlet, d = doublet, t = triplet, q = quartet. [b] Shifts relative to external Me_4Si. [c] Shifts relative to external $BF_3{\cdot}OEt_2$. [d] Since relaxation of carbon or lithium without H is much lower than that of a CH, the relative areas of cage carbons, ferrocene amine, bipyridine, bipyrimidine, and terpyridine units could not be measured accurately.

($SiMe_3$)-3-(Me)-2,3-$C_2B_4H_4$ (**II**) (1.30 g, 4.70 mmol) or 1-Sn-2-($SiMe_3$)-3-(H)-2,3-$C_2B_4H_4$ (**III**) (2.31 g, 8.71 mmol) was reacted with $GeCl_4$ (1.61 g (7.50 mmol) or 2.99 g (13.93 mmol)) to give *closo*-1-Ge-2-($SiMe_3$)-3-(Me)-5-($GeCl_3$)-2,3-$C_2B_4H_3$ (**V**) (0.43 g, 1.05 mmol; 22% yield; mp 91 °C) or *closo*-1-Ge-2-($SiMe_3$)-3-(H)-5-($GeCl_3$)-2,3-$C_2B_4H_3$ (**VI**) (1.77 g, 4.45 mmol; 51% yield; mp 78 °C). The B−$GeCl_3$-substituted germacarboranes **IV**−**VI** are moderately air stable and highly soluble in benzene, THF, and other polar organic solvents but less soluble in *n*-hexane. Anal. Calcd for $C_8H_{21}B_4Cl_3Ge_2Si_2$ (**IV**): C, 20.52; H, 4.53. Found: C, 20.74; H, 4.57. Anal. Calcd for $C_6H_{15}B_4Cl_3Ge_2Si$ (**V**): C, 17.57; H, 3.69. Found: C, 17.52; H, 3.62. Anal. Calcd for $C_5H_{13}B_4Cl_3Ge_2Si$ (**VI**): C, 15.16; H, 3.31. Found: C, 15.43; H, 3.40. The NMR and IR spectral data for **IV**, **V**, and **VI** are given in Tables 1 and 2. Since compounds **IV**−**VI** were the starting materials for the syntheses of all other germacarboranes, the yields of their reactions were maximized; it was found that a 1.6:1 $GeCl_4$-to-stannacarborane molar ratio afforded the highest yields of the Ge(IV)-substituted germacarboranes, the yields reported for **V** and **VI** are for these stiochiometries.

Synthesis of 1-Ge($C_{10}H_8N_2$)-2-($SiMe_3$)-3-(R)-5-($GeCl_3$)-2,3-$C_2B_4H_3$ (R = $SiMe_3$ (VII) and Me (VIII)), 1,1′-(2,2′-$C_8H_6N_4$)-[1-Ge-2-($SiMe_3$)-3-(R)-5-($GeCl_3$)-2,3-$C_2B_4H_3$]$_2$ (R = $SiMe_3$ (IX) and Me (X)), and 1-Ge($C_{15}H_{11}N_3$)-2,3-($SiMe_3$)$_2$-5-($GeCl_3$)-2,3-$C_2B_4H_3$ (XI). The base−germacarbonane complexes **VII**−**XI**, were all synthesized using essentially the same stoichiomteries and reaction conditions. Therefore, only the syntheses of **VII** and **VIII** will be described, with only the yields and analyses of the other complexes detailed. The NMR and IR spectral data for **VII**−**XI** are given in Tables 1 and 2.

closo-1-Ge-2,3-($SiMe_3$)$_2$-5-($GeCl_3$)-2,3-$C_2B_4H_3$ (**IV**) (0.50 g, 1.06 mmol) or *closo*-1-Ge-2-($SiMe_3$)-3-(Me)-5-($GeCl_3$)-2,3-$C_2B_4H_3$ (**V**) (0.50 g, 1.23 mmol) was dissolved in freshly distilled dry benzene (15 mL) in vacuo. This solution was then filtered through a glass frit under high vacuum onto freshly sublimed

Table 2. FT-IR Spectral Data[a] for *closo*-Germacarboranes and Their Donor−Acceptor Complexes (IV−XI) and Related Derivatives (XII and XIII) (C_6D_6 vs C_6D_6)

compd	wavenumber (cm^{-1})
IV	2945(s,s), 2900(sh), 2840(sh)[ν(C−H)], 2575(sh)[ν(B−H)], 1400(sh), 1310(wbr) [$\delta(CH)_{asym}$], 1250(s)[$\delta(CH)_{sym}$], 1160(wbr), 977(wbr), 830(vsbr)[ρ(CH)], 720(wbr), 620(wbr), 525(wbr), 441(s,s), 382(sbr)
V	2955(vs), 2925(sh), 2900(sh), 2860(ws)[ν(C−H)], 2585(vvs)[ν(B−H)], 1445(ws), 1410(ws), 1380(ws), 1325(wbr)[$\delta(CH)_{asym}$], 1255(vvs) [$\delta(CH)_{sym}$], 1205(vs), 1088(sh), 1058(vs), 1020(ms), 985(ms), 950(ws), 845(vvs)[ρ(CH)], 820(ms), 795(sh), 625(ms), 562(ws), 518(ms), 425(ms), 400(vvs), 333(ws)
VI	2955(vvs), 2898(ms)[ν(C−H)], 2595(vvs)[ν(B−H)], 1945(wbr), 1877(wbr), 1465(ws), 1410(ms), 1360(mbr), 1309(wbr)[$\delta(CH)_{asym}$], 1255(vvs) [$\delta(CH)_{sym}$], 1190(sh), 1168(ms), 1122(ms), 1072(m), 992(ms), 980(ms), 951(ms), 897(ms), 840(vvs)[ρ(CH)], 760(vs), 698(ms), 620(vs), 550(ws), 445(vs), 410(sh), 390(vvs), 332(ws), 300(wbr)
VII	2964(vs), 2926(ms), 2862(m)[ν(C−H)], 2555(vs)[ν(B−H)], 2395(m), 2280 (vs)[ν(C═N)], 1628(m), 1603(m), 1443(ms), 1328(vs)[$\delta(CH)_{asym}$], 1251(vs)[$\delta(CH)_{sym}$], 1219(m), 1155(m), 1098(mbr), 1021(vs), 983(w), 842(vs) [ρ(CH)], 812(vs), 769(ms), 638(ws), 520(ms), 505(vs), 465(ms)
VIII	3092(vss), 3065(vss), 3032(vs), 2960(vs), 2887(ms)[ν(C−H)], 2552(vs) [ν(B−H)], 2394(ms), 2335(ms), 2288(vs)[ν(C═N)], 1966(vs), 1821(vs), 1755(ws), 1676(ws), 1610(ms), 1531(ms), 1485(vs), 1393(ms), 1340 (ms), 1314(ms)[$\delta(CH)_{asym}$], 1255(vs) [$\delta(CH)_{sym}$], 1023(vs), 840(vs) [ρ(CH)], 814(vs), 761(vs), 675(vvs), 432(ms)
IX	3100(vs), 3075(vs), 3044(vs), 2962(ms), 2886(ms)[ν(C−H)], 2553(vs,br) [ν(C−H)], 2384(ms), 2321(ms), 2284(vs)[ν(C═N)], 1963(vs), 1819(vs), 1618(ms), 1486(ms), 1417(vs), 1335(vs) [$\delta(CH)_{asym}$], 1272(vs) [$\delta(CH)_{sym}$], 1090(sh), 1040(vs), 852(vs)[ρ(CH)], 820(vs), 688(ms, br)
X	3107(vs), 3041(vs), 2962(vs), 2903(sh)[ν(C−H)], 2594(s)[ν(C−H)], 2397(ws), 2305(ms), 2240(ms), 1963(vs), 1812(vs), 1484(vs), 1110(s), 1024(vs), 827(s)[ρ(CH)], 689(vs), 669(s)
XI	3098(vs), 3079(vs), 3033(vs), 2954(ws), 2901(w)[ν(C−H)], 2565(m,br) [ν(C−H)], 1960(ws), 1815(ms), 1618(w), 1479(vs), 1262(ms), 1038(vs), 848(ms)[ρ(CH)], 775(m), 676(vs), 459(ws), 406(ms)
XII	3098(ss)[ν(C−N)], 2960(vs), 2887(ss)[ν(C−H)], 2360(ws), 2335(ms), 2291(ms), 2228(ms), 1992(ms), 1915(ms), 1852(ms), 1741(ms), 1658(ms), 1463(vs), 1359(ss) [$\delta(CH)_{asym}$], 1331(ws), 1297(sh), 1241(ms)[$\delta(CH)_{sym}$], 1199(ss), 1074(ss), 907(ss), 840(vs)[ρ(CH)], 636(ws), 595(ms), 490(ss)
XIII	3092(ss)[ν(C−N)], 2954(vs), 2926(vs), 2891(ss)[ν(C−H)], 2793(sh), 2552(vs) [ν(B−H)], 2465(ms), 2395(ws), 2298(ms), 1907(sbr), 1768(ss), 1718(ms), 1656(ms), 1516(ss), 1454(ss), 1412(ss), 1349(ms) [$\delta(CH)_{asym}$], 1251(vs)[$\delta(CH)_{sym}$], 1063(ws), 840(vs)[ρ(CH)], 679(ms), 491(ss)

[a] Legend: v = very, s = strong or sharp, m = medium, w = weak, sh = shoulder, and br = broad.

anhydrous 2,2′-bipyridine, $C_{10}H_8N_2$ (0.17 g (1.06 mmol) or 0.19 g (1.23 mmol)), dissolved in 5 mL of dry benzene at 0 °C. The resulting solution was stirred constantly for 3 days at room temperature, during which time the originally red-colored homogeneous mixture turned to orange-brown and slowly became turbid. The solvent, benzene, was then removed from the solution in vacuo, and the dark orange residue that remained in the flask was heated to 60 °C to remove the unreacted 2,2′-bipyridine (0.052 g (0.33 mmol) or 0.064 g (0.41 mmol)), which was collected in a detachable U-trap held at −196 °C. The resulting dark residue left behind in the reaction flask was then extracted with a 5:1 mixture of *n*-hexane and benzene. After removal of solvents from the extract, a red microcrystalline solid was obtained, which was later recrystallized from benzene to produce bright-red platelike crystals of 1-Ge($C_{10}H_8N_2$)-2,3-($SiMe_3$)$_2$-5-($GeCl_3$)-2,3-$C_2B_4H_3$ (**VII**) (0.42 g, 0.67 mmol; 63% yield; mp 134 °C) or 1-Ge($C_{10}H_8N_2$)-2-($SiMe_3$)-3-(Me)-5-($GeCl_3$)-2,3-$C_2B_4H_3$ (**VIII**) (0.41 g, 0.72 mmol; 59% yield; mp 130 °C). Anal. Calcd for $C_{18}H_{29}B_4Cl_3N_2Ge_2Si_2$ (**VII**): C, 34.62; H, 4.55; N, 4.46. Found: C, 34.90; H, 4.69; N, 4.49. Anal. Calcd for $C_{16}H_{23}B_4Cl_3N_2Ge_2Si$ (**VIII**): C, 33.94; H, 4.09; N, 4.95. Found: C, 34.08; H, 4.16; N, 5.05.

In a like manner, **IV** (0.68 g, 1.45 mmol) or **V** (0.61 g, 1.47 mmol) was reacted with 2,2′-bipyrimidine, $C_8H_6N_4$ (0.230 g (1.45 mmol) or 0.232 g (1.47 mmol), when R = $SiMe_3$ or Me, respectively), to give unreacted $C_8H_6N_4$ (0.175 g (1.11 mmol) or 0.153 g (0.97 mmol), for **IV** and **V**, respectively) and, after extraction with 5:1 *n*-hexane and benzene and recrystallization from benzene, yellow-orange needlelike crystals of 1,1′-(2,2′-$C_8H_6N_4$)-[1-Ge-2,3-($SiMe_3$)$_2$-5-($GeCl_3$)-2,3-$C_2B_4H_3$]$_2$ (**IX**) (0.32 g, 0.29 mmol; 40% yield; mp 189 °C (dec)) and 1,1′-(2,2′-$C_8H_6N_4$)-[1-Ge-2-($SiMe_3$)-3-(Me)-5-($GeCl_3$)-2,3-$C_2B_4H_3$]$_2$ (**X**) (0.40 g, 0.41 mmol; 56% yield; mp 182 °C (dec)), respectively. Anal. Calcd for $C_{24}H_{48}B_8Cl_6N_4Ge_4Si_4$ (**IX**): C, 26.34; H, 4.42; N, 5.12. Found: C, 26.54; H, 4.38; N, 4.95. Anal. Calcd for $C_{20}H_{36}B_8Cl_6N_4Ge_4Si_2$ (**X**): C, 24.55; H, 3.71; N, 5.73. Found: C, 24.93; H, 3.82; N, 5.75.

In the synthesis of **XI**, 0.41 g (0.88 mmol) of **IV** was reacted with 0.22 g (0.89 mmol) of 2,2′:6′,2″-terpyridine, $C_{15}H_{11}N_3$, to give 0.016 g (0.26 mmol) of unreacted $C_{15}H_{11}N_3$ and, after extraction with *n*-hexane, a green solid that was later identified as 1-Ge($C_{15}H_{11}N_3$)-2,3-($SiMe_3$)$_2$-5-($GeCl_3$)-2,3-$C_2B_4H_3$ (**XI**) (0.41 g, 0.57 mmol; 67% yield; mp 124 °C (dec)). Anal. Calcd for $C_{23}H_{32}B_4Cl_3N_3Ge_2Si_2$ (**XI**): C, 39.38; H, 4.60; N, 5.99. Found: C, 39.13; H, 4.30; N, 6.28.

Attempted Synthesis of 1-Ge[(η^5-C_5H_5)Fe(η^5-$C_5H_4CH_2$-($Me)_2$N)]-2,3-($SiMe_3$)$_2$-5-($GeCl_3$)-2,3-$C_2B_4H_3$: Syntheses of {[(η^5-C_5H_5)Fe(η^5-$C_5H_4CH_2$]$_2$N($Me)_2$}$^+$[$GeCl_3$]$^-$ (XII) and 1-Ge[(η^5-C_5H_5)Fe(η^5-$C_5H_4CH_2$($Me)_2$N)]-2,3-($SiMe_3$)$_2$-5-(NMe_2)-2,3-$C_2B_4H_3$ (XIII). The *closo*-germacarborane **IV** (0.7 g, 1.49 mmol) was dissolved in 15 mL of dry benzene in vacuo, and the resulting solution was poured onto freshly distilled anhydrous (ferrocenylmethyl)-*N*,*N*-dimethylamine, [(η^5-C_5H_5)-Fe(η^5-$C_5H_4CH_2$($Me)_2$N)] (0.72 g, 2.98 mmol), contained in a reaction flask that was immersed in a −78 °C bath. After warming the reaction flask to room temperature, the solution was stirred for 4 days, during which time the color turned to bright orange and the solution slowly became turbid. The solvent, benzene, and any trace quantity of unreacted (ferrocenylmethyl)-*N*,*N*-dimethylamine were removed from the reaction mixture by pumping over a period of 18 h at room temperature, leaving behind a bright orange, gummy solid in the flask. The solid was washed twice with dry *n*-hexane (20 mL) in vacuo, dissolved in dry benzene (35 mL), and the resulting bright-orange solution was allowed to stand in a cool place for several days, during which time a substantial quantity of yellow-orange crystals were isolated. These crystals were later identified as the salt, {[(η^5-C_5H_5)Fe(η^5-C_5H_4-CH_2]$_2$N($Me)_2$}$^+$[$GeCl_3$]$^-$ (**XII**; 0.42 g, 0.68 mmol; 46% based on **IV** consumed; mp 110 °C). After complete removal of **XII**, the bright orange-colored mother liquor was further concentrated to check whether any new crystals would form. Since further crystallization did not occur, even after standing in a cool place for 7−8 days, the remaining benzene solvent was removed in vacuo to collect an orange residue at the bottom of the flask. This residue was slowly dried at 120 °C in vacuo over a period of 8 h and then recrystallized from a benzene/hexane (1:1) solution to isolate a microcrystalline orange solid, identified as 1-Ge[(η^5-C_5H_5)Fe(η^5-$C_5H_4CH_2$($Me)_2$N)]-2,3-($SiMe_3$)$_2$-5-(NMe_2)-2,3-$C_2B_4H_3$ (**XIII**), in 48% yield (0.41 g, 0.71 mmol). At room temperature, **XII** was highly soluble in THF but only slightly soluble in benzene and *n*-hexane. On the other hand, **XIII**

was highly soluble in either THF or benzene but sparingly soluble in *n*-hexane. Anal. Calcd for $C_{24}H_{28}Cl_3NFe_2Ge$ (**XII**): C, 46.41; H, 4.54; N, 2.26. Found (duplicate runs): C, 45.50 and 46.57; H, 4.51 and 5.46; N, 2.17 and 2.16. Anal. Calcd for $C_{23}H_{44}B_4N_2FeGeSi_2$ (**XIII**): C, 47.92; H, 7.69; N, 4.86. Found: C, 48.17; H, 7.79; N, 5.04. The NMR and IR spectral data for **XII** and **XIII** are given in Tables 1 and 2.

X-ray Analysis of *closo*-1-Ge-2-(SiMe$_3$)-3-(R)-5-(GeCl$_3$)-2,3-C$_2$B$_4$H$_3$ (R = SiMe$_3$ (IV), Me (V), and H (VI)), 1-Ge-(C$_{10}$H$_8$N$_2$)-2,3-(SiMe$_3$)$_2$-5-(GeCl$_3$)-2,3-C$_2$B$_4$H$_3$ (VII), 1,1′-(2,2′-C$_8$H$_6$N$_4$)-[1-Ge-2,3-(SiMe$_3$)$_2$-5-(GeCl$_3$)-2,3-C$_2$B$_4$H$_3$]$_2$ (IX), and {[(η^5-C$_5$H$_5$)Fe(η^5-C$_5$H$_4$CH$_2$]$_2$N(Me)$_2$}$^+$[GeCl$_3$]$^-$ (XII). Suitable colorless, transparent crystals of *closo*-1-Ge-2-(SiMe$_3$)-3-(R)-5-(GeCl$_3$)-2,3-C$_2$B$_4$H$_3$ (**IV**−**VI**) were grown from their respective solutions of benzene/hexane (1:1), red platelike crystals of **VII** and orange needle-shaped crystals of **IX** were grown very slowly from their respective benzene solutions, while orange plate-shaped crystals of **XII** were obtained by slow crystallization from its solution of benzene and THF (5:1). The crystals were coated with an epoxy resin and mounted sequentially on a Seimens R3m/V diffractometer with Mo Kα radiation. The pertinent crystallographic data are summarized in Table 3. Final unit cell parameters were obtained by a least-squares fit of the angles of 24 accurately centered reflections in the range $3.5° \le 2\theta \le 44.0°$ for **IV**−**VI** and **XII** and $5.0° \le 2\theta \le 30.0°$ for **VII** and **IX**. Intensity data were collected at 230 K (220 K for **XII**) in the range of $3.0° \le 2\theta \le 50°$ (**IV**), $3.5° \le 2\theta \le 45.0°$ (**V**), $3.5° \le 2\theta \le 44.0°$ (**VI**), $3.5° \le 2\theta \le 42.0°$ (**VII**), $3.0° \le 2\theta \le 40.0°$ (**IX**), or $3.5° \le 2\theta \le 44.0°$ (**XII**). Three standard reflections, monitored after every 200 (**IV**−**VI**), 300 (**IX**), or 100 (**XII**) reflections, did not show any significant change in intensity during the data collection. A total of 3804 (**IV**), 2935 (**V**), 2057 (**VI**), 4281 (**VII**), 5166 (**IX**), or 1784 (**XII**) independent reflections were collected. These data were corrected for Lorentz and polarization effects; semiempirical absorption corrections (ψ scans) were applied for each structure. The structures were solved by direct methods and subsequent difference Fourier syntheses using the *SHELXTL-Plus* package.[20] All non-hydrogen atoms were refined anisotropically. Cage hydrogen atoms were located in difference Fourier maps and included in the refinement with fixed position and isotropic thermal parameters, while the 2,2′-bipyridine and 2,2′-bipyrimidine H's were in calculated positions. The scattering factors, with anomalous dispersion corrections for Cl and Ge in each structure, were taken from ref 21. The final full-matrix least-squares refinement using 2818 (**IV**), 1951 (**V**), 1258 (**VI**), 2365 (**VII**), and 2243 (**IX**) reflections with $[F > 6.0\sigma(F)]$ or 1446 reflections with $[F > 4.0\sigma(F)]$ (**XII**) converged to $R = 0.040$ (**IV**), 0.031 (**V**), 0.045 (**VI**), 0.032 (**IX**), or $R = 0.060$ (**XII**) and $R_w = 0.044$ (**IV**), 0.037 (**V**), 0.056 (**VI**), 0.039 (**VII**), 0.058 (**IX**), or 0.068 (**XII**). The GOF parameters for the compounds are listed in Table 3. The atomic coordinates are given in the Supporting Information, while selected interatomic distances and angles are listed in Table 4.

Calculations. Approximate density functional theory (DFT) and Hartree−Fock (HF) ab initio molecular orbital calculations at several different levels of theory were carried out on either a Dec-αA or Silicon Graphics Indigo2 RS10000 workstation, using the Gaussian 94 series of programs.[22] Most of the calculations were conducted on the model compounds 1,2,3-GeC$_2$B$_4$H$_6$ (**XIV**) and 5-GeCl$_3$-1,2,3-GeC$_2$B$_4$H$_5$ (**XV**) in which H's replace the SiMe$_3$ groups on the cage carbons. It has been shown that these model compounds provide very useful information concerning the structures and properties of the trimethylsilyl-substituted metallacarboranes.[23] Boron-11 NMR chemical shifts of the model compounds were obtained using gauge-independent atomic orbital (GIAO)[24] calculations at the HF/6-311G** level on structures optimized using Becke's three-parameter hybrid methods[25] and the correlation functional of Lee, Yang, and Parr[26] at the 6-31G* level of theory (GIAO-HF/6-311G**//B3LYP/6-31G*). Such calculations have been found to give reliable ^{13}C and ^{11}B NMR chemical shifts in a number of carbon- and boron-containing compounds.[23,27] The ^{11}B NMR chemical shifts are relative to the BF$_3$·OEt$_2$ standard. In all cases, the standard was subjected to the same optimization/GIAO cycle as the particular compound.

Results and Discussion

Syntheses. Anhydrous GeCl$_4$ was found to react with the *closo*-stannacarboranes 1-Sn-2-(SiMe$_3$)-3-(R)-2,3-C$_2$B$_4$H$_4$ (R = SiMe$_3$ (**I**), Me (**II**), and H (**III**)) in the absence of solvents to give the corresponding germacarboranes 1-Ge-2-(SiMe$_3$)-3-(R)-5-(GeCl$_3$)-2,3-C$_2$B$_4$H$_3$ (R = SiMe$_3$ (**IV**), Me (**V**), and H (**VI**)) in yields of 43%, 22%, and 51%, respectively, based on the stannacarborane consumed.[8] A detailed product analysis in the synthesis of **IV** showed that a 1:1 GeCl$_4$-to-stannacarborane stoichiometric ratio produced roughly 0.5 mol of the neutral carborane precursor for every mole of the GeCl$_3$-substituted germacarborane formed. Formally, the substitution of the terminal H on the unique boron by a GeCl$_3$ group would liberate an HCl molecule, which could then react with another stannacarborane to give, ultimately, SnCl$_2$ and the neutral *nido*-carborane. On this basis, one would expect 0.5 mol of the neutral carborane to be produced for each mole of the GeCl$_3$-substituted germacarborane formed; this was found to be the case in the formation of **IV**. Another side product, formed in 29% yield, was *commo*-1,1′-Ge-[2,3-(SiMe$_3$)$_2$-2,3-C$_2$B$_4$H$_4$]$_2$. The product distributions in these reactions were found to be sensitive to the beginning reactant stoichiometries as well as temperature. Earlier work in our laboratories had shown that the reaction of GeCl$_4$ with stannacarborane (**I**) in a 1:2 molar ratio, in the absence of solvent and at 150−160 °C, produced only *commo*-1,1′-Ge-[2,3-(SiMe$_3$)$_2$-2,3-C$_2$B$_4$H$_4$]$_2$ in 74% yield.[28] A lower temperature (135 °C) and a higher GeCl$_4$-to-stannacarborane (**I**) molar ratio (1:1) gave the product distribution described in the Experimental Section. It was found that a 1.6:1 GeCl$_4$-to-stannacarborane molar ratio and a reaction temperature of 135 °C afforded the highest net yield of the Ge(IV)-substituted germacarborane (**IV**). These were the reaction conditions used in the production of **V** and **VI**.

(20) Sheldrick, G. M. *Structure Determination Software Programs;* Siemens X-ray Analytical Instrument Corp.: Madison, WI, 1991.
(21) *International Tables For X-ray Crystallography*; Kynoch Press: Birmingham, U.K., 1974; Vol. IV.
(22) Frisch, M. J.; Trucks, G. W.; Schlegel, H. B.; Gill, P. M. W.; Johnson, B. F. G.; Robb, M. A.; Cheeseman, J. R.; Keith, T.; Peterson, G. A.; Montgomery, J. A.; Raghavachari, K.; Al-Laham, M. A.; Zakrzewski, V. G.; Ortiz, J. V.; Foresman, J. B.; Peng, C. Y.; Ayala, P. Y.; Chen, W.; Wong, M. W.; Andres, J. L.; Replogle, E. S.; Gomperts, R.; Martin, R. L.; Fox, D. J.; Binkley, J. S.; Defrees, D. J.; Baker, J.; Stewart, J. P.; Head-Gordon, M.; Gonzalez, C.; Pople, J. A. *Gaussian 94, Revision B.3*; Gaussian, Inc.: Pittsburgh, PA, 1995.
(23) (a) Ezhova, M. B.; Zhang, H.; Maguire, J. A.; Hosmane, N. S. *J. Organomet. Chem.* **1998**, *550*, 409. (b) Hosmane, N. S.; Lu, K.-J.; Zhang, H.; Maguire, J. A. *Organometallics* **1997**, *16*, 5163.
(24) Wolinski, K.; Hilton, J. F.; Pulay, P. *J. Am. Chem. Soc.* **1990**, *112*, 8251.
(25) Becke, A. D. *J. Chem. Phys.* **1993**, *98*, 5648.
(26) Lee, C.; Yang, W.; Parr, R. G. *Phys. Rev.* **1988**, *B37*, 785.
(27) Cheeseman, J. R.; Trucks, G. W.; Keith, T. A.; Frisch, M. J. *J. Chem. Phys.* **1996**, *104*, 5497.
(28) Hosmane, N. S.; Barreto, R. D.; Tolle, M. A.; Alexander, J. J.; Quintana, W.; Siriwardane, U.; Shore, S. G.; Williams, R. E. *Inorg. Chem.* **1990**, *29*, 2698.

Table 3. Crystallographic Data

	$GeCl_3$-substituted *closo*-germacarboranes			donor−acceptor complexes of $GeCl_3$-substituted germacarboranes		$\{[(\eta^5\text{-}C_5H_5)Fe(\eta^5\text{-}C_5H_4CH_2)]_2N(Me)_2\}^+[GeCl_3]^-$
	IV	**V**	**VI**	**VII**	**IX**	**(XII)**
formula	$C_8H_{21}B_4Si_2Cl_3Ge_2$	$C_6H_{15}B_4SiCl_3Ge_2$	$C_5H_{13}B_4SiCl_3Ge_2$	$[C_{18}H_{29}B_4N_2Si_2Cl_3Ge_2]\cdot 1.5[C_6H_6]$	$[C_{24}H_{48}B_8N_4Si_4Cl_6Ge_4]\cdot [C_6H_6]$	$C_{24}H_{28}Cl_3NGeFe_2$
fw	468.2	410.0	396.0	741.5	1172.7	621.1
cryst syst	triclinic	monoclinic	monoclinic	monoclinic	monoclinic	
space group	$P\bar{1}$	$P2_1/c$	$P2_1/c$	$P2_1/c$	$C2/c$	$P2_12_12_1$
a, Å	6.845 (4)	14.635(3)	11.735(4)	19.480(3)	52.361(11)	7.536(10)
b, Å	11.815 (8)	8.770(3)	10.488(3)	14.192(3)	12.184(3)	14.544(2)
c, Å	12.898 (5)	13.887(3)	13.500(5)	13.276(3)	12.868(4)	23.065(3)
α, deg	89.47 (4)	90	90			
β, deg	87.46 (4)	111.14(2)	106.70(2)	94.48(1)	99.33(2)	
γ, deg	81.82 (5)	90	90			
V, Å^3	1031.6 (9)	1662.5(8)	1591.5(9)	3658(1)	10628(5)	2528.0(6)
Z	2	4	4	4	8	4
D_{calcd}, Mg·m^{-3}	1.51	1.638	1.653	1.346	1.466	1.632
abs coeff, mm^{-1}	3.37	4.140	4.322	1.948	2.660	2.644
cryst dimns, mm	0.15 × 0.25 × 0.20	0.15 × 0.25 × 0.20	0.20 × 0.30 × 0.15	0.35 × 0.25 × 0.10	0.10 × 0.15 × 0.30	
scan type	ω	ω	ω	ω	ω	
scan sp in ω; min, max				5.0, 30.0	5.0, 30.0	
2θ range, deg	3−50	3.5−45.0	3.5−44.0	3.5−42.0	3.0−40.0	3.5−44.0
T, K	298	230	230	230	230	220
decay, %	0	0	0	0	0	
no. of data collected	3804	2935	2057	4281	5166	1784
no. of obsd reflns, $F > 6.0\sigma(F)$	2818	1951	1258	2365	2243	1446
no. of params refined	150	150	147	363	316	280
GOF	2.13	1.32	1.29	0.88	1.17	1.46
$\Delta\rho_{(max, min)}$, e/Å^3				0.25, −0.25	0.76, −0.48	
R^b	0.040	0.031	0.045	0.032	0.051	0.0596
wR	0.044	0.037	0.056	0.039	0.058	0.0680

[a] Graphite-monochromatized Mo Kα radiation, $\lambda = 0.71073$ Å. [b] $R = \sum||F_o| - |F_c||/\sum|F_o|$, $wR = [\sum w(F_o - F_c)^2/\sum w(F_o)^2]^{1/2}$, and $w = 1/[\sigma^2(F_o) + g(F_o)^2]$.

Table 4. Selected Bond Lengths (Å) and Bond Angles (deg)

	Bond Lengths		
	Compound IV		
Ge(1)−C(1)	2.251 (4)	Ge(1)−C(2)	2.244 (4)
Ge(1)−B(3)	2.265 (6)	Ge(1)−B(4)	2.243 (6)
Ge(1)−B(5)	2.250 (6)	Ge(2)−Cl(1)	2.141 (2)
Ge(2)−Cl(2)	2.154 (2)	Ge(2)−Cl(3)	2.139 (2)
Ge(2)−B(4)	1.995 (6)		
	Compound V		
Ge(1)−Cnt	1.185	Ge(1)−C(11)	2.286 (5)
Ge(1)−C(12)	2.267 (5)	Ge(1)−B(13)	2.270 (6)
Ge(1)−B(14)	2.234 (6)	Ge(1)−B(15)	2.272 (5)
Ge(2)−Cl(1)	2.154 (2)	Ge(2)−Cl(2)	2.144 (2)
Ge(2)−Cl(3)	2.147 (2)	Ge(2)−B(14)	1.996 (6)
	Compound VI		
Ge(1)−Cnt	1.823	Ge(1)−C(11)	2.272 (10)
Ge(1)−C(12)	2.261(10)	Ge(1)−B(13)	2.276 (12)
Ge(1)−B(14)	2.240 (11)	Ge(1)−B(15)	2.262 (12)
Ge(2)−Cl(1)	2.130 (4)	Ge(2)−Cl(2)	2.128 (4)
Ge(2)−Cl (3)	2.131 (4)	Ge(2)−B(14)	1.996 (10)
	Compound VII		
Ge(1)−C(11)	2.761 (6)	Ge(1)−C(12)	2.806 (6)
Ge(1)−B(13)	2.443 (7)	Ge(1)−B(14)	2.173 (7)
Ge(1)−B(15)	2.407 (7)	Ge(1)−N(31)	2.225 (5)
Ge(1)−N(38)	2.205 (5)	Ge(2)−Cl(1)	2.159 (2)
Ge(2)−Cl(2)	2.179 (2)	Ge(2)−Cl(3)	2.166 (2)
Ge(2)−B(14)	2.005 (7)		
	Compound IX		
Ge(1)−C(11)	2.577	Ge(1)−C(12)	2.565
Ge(1)−B(13)	2.337 (20)	Ge(1)−B(14)	2.193 (19)
Ge(1)−B(15)	2.308 (20)	Ge(1)−N(51)	2.531 (13)
Ge(1)−N(58)	2.543 (13)	Ge(3)−Cl(1)	2.124 (7)
Ge(3)−Cl(2)	2.151 (5)	Ge(3)−Cl(3)	2.160 (7)
Ge(3)−B(14)	1.986 (20)	Ge(2)−C(21)	2.445 (15)
Ge(2)−C(22)	2.443 (16)	Ge(2)−B(23)	2.284 (19)
Ge(2)−B(24)	2.200 (18)	Ge(2)−B(25)	2.303 (20)
Ge(2)−N(55)	2.699 (14)	Ge(2)−N(62)	2.606 (13)
Ge(4)−Cl(4)	2.163 (6)	Ge(4)−Cl(5)	2.160 (50)
Ge(4)−Cl(6)	2.117 (7)	Ge(4)−B(24)	2.008 (20)
	Compound XII		
Ge−Cl(1)	2.287(5)	Ge−Cl(2)	2.281 (6)
Ge−Cl(3)	2.276 (4)	C(51)−N(53)	1.517(15)
C(52)−N(53)	1.544(14)	N(53)−C(54)	1.506(14)
N(53)−C(54)	1.521(16)	Ge−N(53)	5.425 (10)
Ge−C(51)	4.733 (14)	Ge−C(52)	4.947 (12)
	Bond Angles		
	Compound IV		
C(1)−Ge(1)−C(2)	38.9 (2)	C(2)−Ge(1)−B(3)	41.1 (2)
B(1)−Ge(1)−B(4)	43.0 (2)	C(1)−Ge(1)−B(5)	40.9 (2)
B(4)−Ge(1)−B(5)	43.2 (2)	C(1)−B(6)−C(2)	51.6 (3)
C(2)−B(6)−B(3)	53.5 (3)	B(3)−B(6)−B(4)	55.5 (3)
C(1)−B(6)−B(5)	53.6 (3)	B(4)−B(6)−B(5)	55.9 (3)
Cl(1)−Ge(2)−Cl(2)	103.4 (1)	Cl(1)−Ge(2)−Cl(3)	102.8 (1)
Cl(2)−Ge(2)−Cl(3)	104.1 (1)		
	Compound V		
C(11)−Ge(1)−C(12)	38.2 (1)	C(12)−Ge(1)−B(13)	40.3 (2)
B(13)−Ge(1)−B(14)	43.8 (2)	C(11)−Ge(1)−B(15)	40.7 (2)
B(14)−Ge(1)−B(15)	43.4 (2)	C(11)−B(16)−C(12)	50.4 (3)
C(12)−B(16)−B(13)	52.5 (3)	B(13)−B(16)−B(14)	56.6 (3)
C(11)−B(16)−B(15)	52.8 (3)	B(14)−B(16)−B(15)	55.8 (3)
Cl(1)−Ge(2)−Cl(2)	104.2(1)	Cl(1)−Ge(2)−Cl(3)	103.8(1)
Cl(2)−Ge(2)−Cl(3)	104.1(1)		
	Compound VI		
C(11)−Ge(1)−C(12)	37.7 (3)	C(12)−Ge(1)−B(13)	39.7 (4)
B(13)−Ge(1)−B(14)	42.8 (4)	C(11)−Ge(1)−B(15)	39.9 (3)
B(14)−Ge(1)−B(15)	43.9 (4)	C(11)−B(16)−C(12)	51.0 (6)
C(12)−B(16)−B(13)	52.7 (6)	B(13)−B(16)−B(14)	55.7 (7)
C(11)−B(16)−B(15)	52.1 (6)	B(14)−B(16)−B(15)	56.8 (7)
Cl(1)−Ge(2)−Cl(2)	103.8(1)	Cl(1)−Ge(2)−Cl(3)	103.9(1)
Cl(2)−Ge(2)−Cl(3)	103.9(1)		
	Compound VII		
Cnt−Ge(1)−N(31)	121.2	Cnt−Ge(1)−N(38)	122.7
	Compound IX		
Cnt(1)−Ge(1)−N(51)	122.3	Cnt(1)−Ge(1)−N(58)	120.3
	Compound XII		
Cl(1)−Ge−Cl(2)	95.2 (2)	Cl(1)−Ge−Cl(3)	96.3(2)
Cl(2)−Ge−Cl(3)	94.3 (1)	C(51)−N(53)−C(54)	112.1 (9)
C(51)−N(53)−C(52)	105.2 (8)	C(54)−N(53)−C(55)	109.4 (9)
C(52)−N(53)−C(55)	110.3 (9)		

Scheme 1 summarizes the reactions leading to the formation of the germacarboranes. No neutral $GeCl_3$-substituted carborane was found in the reaction products, indicating that the initial step in the reaction sequence was the reductive insertion of germanium into the carborane cage to form a *closo*-germacarborane, which then reacted with a second $GeCl_4$ molecule to give the Ge(IV)-substituted complex and HCl. Such a substitution is not unreasonable from an energy standpoint. For example, ab initio molecular orbital calculations at the B3LYP/6-31G* level produced a ΔE of −20.83 kJ/mol for eq 1. Although this value is only approximate

$$\textit{closo}\text{-}1,2,3\text{-}GeC_2B_4H_6 + GeCl_4 \rightarrow 5\text{-}GeCl_3\text{-}1,2,3\text{-}GeC_2B_4H_5 + HCl \quad (1)$$

and is for the gas phase, it does indicate that the substitution of a $GeCl_3$ unit for a terminal hydrogen should be an energetically favorable process.

As pointed out above, the absence of any neutral $GeCl_3$-substituted *nido*-carboranes indicates that the first step in the reaction sequence leading to the formation of **IV**−**VI** must be the insertion of germanium into the C_2B_4 cage. Since all structural and spectroscopic evidence unequivocally show that the capping germanium atoms in **IV**−**VI** are in formal +2 states, this process must be a reductive insertion. While the identities of the reduction products (**IV**−**VI**) is well-established, the identities of the accompanying oxidation products are not known. Since the reaction of the stannacarboranes with the metal halides $PtCl_4$ and $PtCl_2$ leads to oxidative closure of the carborane cage to give the corresponding *closo*-carboranes and Pt metal[28] and $NiCl_2$ is known to react in a similar fashion with the group 1 compounds of these carboranes,[29] *closo*-carborane formation was thought to be a likely coproduct of the germanium insertion. However, there is no evidence of the formation of a *closo*-carborane among the products in the synthesis of **IV**. In addition, when the reactions were run under conditions similar to those in the present study (160 °C and no solvent), but with an excess of the stannacarborane, the only product found was the corresponding full-sandwich germacarboranes,[30] indicating that any redox process must come after tin substitution. The product analysis in the synthesis of **IV**, as summarized in Scheme 1, shows that the net reaction involves 3 mol of the stannacarborane reacting with 4 mol of $GeCl_4$ to give 2 mol of the $GeCl_3$-substituted germacarborane, 1 mol of the neutral carborane, and 3 mol of $SnCl_2$, which leaves 4 mol of chlorine unaccounted for. These chlorines may be associated with the oxidation products. The formation of the full- and half-sandwich germacarboranes can be understood on the basis of a sequence involving an initial reaction of the stannacarborane with $GeCl_4$ to give $SnCl_2$ and a reactive dichlorogermanium(IV) carborane intermediate in which a $(GeCl_2)^{2+}$ unit replaces an apical Sn(II) in the stannacarborane. In the presence of excess stannacarborane, the intermediate could react

(29) Hosmane, N. S.; Saxena, A. K.; Barreto, R. D.; Zhang, H.; Maguire, J. A.; Jia, L.; Wang, Y.; Oki, A. R.; Grover, K. V.; Whitten, S. J.; Dawson, K.; Tolle, M. A.; Siriwardane, U.; Demissie, T.; Fagner, J. S. *Organometallics* **1993**, *12*, 3001.

(30) Islam, M. S.; Siriwardane, U.; Hosmane, N. S.; Maguire, J. A.; de Meester, P.; Chu, S. S. C. *Organometallics* **1987**, *6*, 1936.

Scheme 1

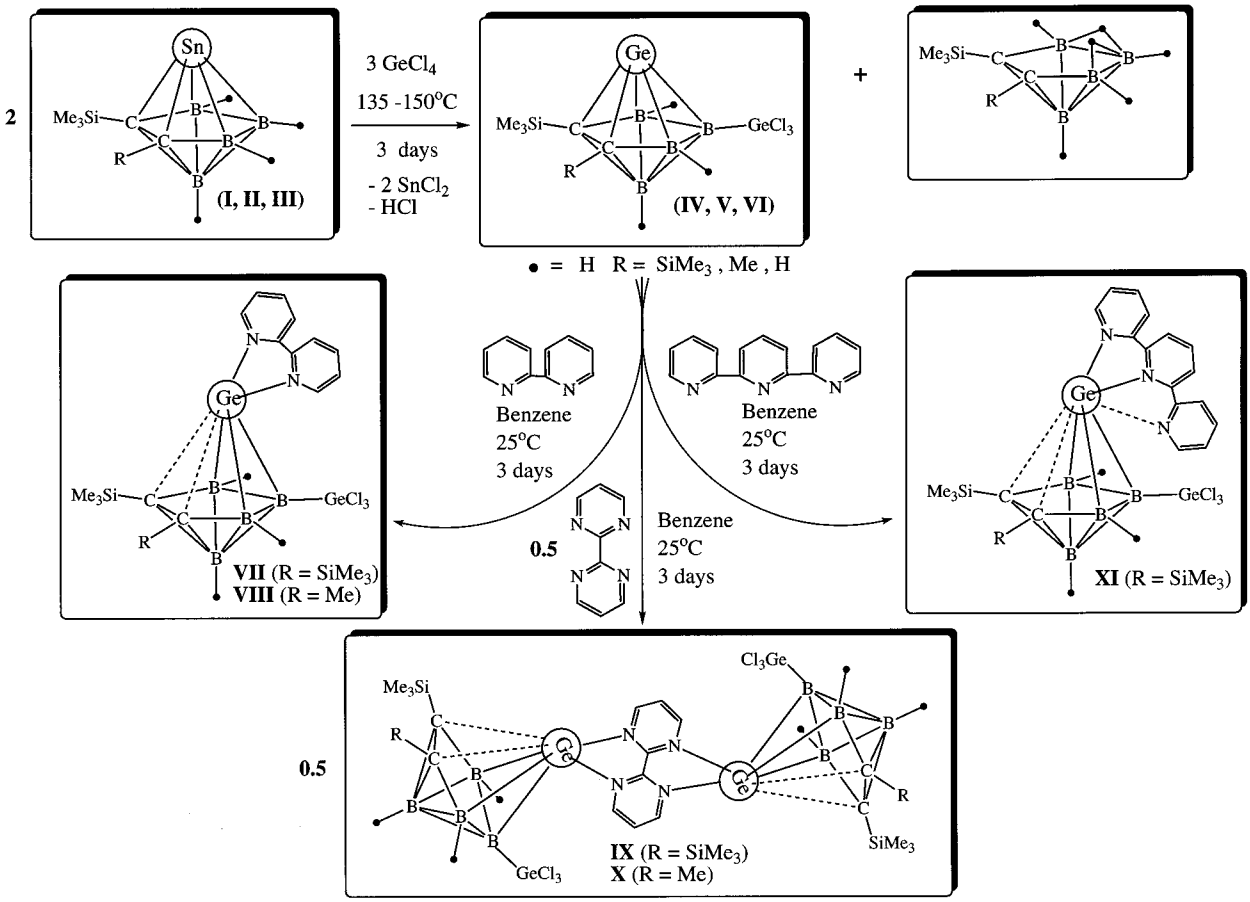

with another stannacarborane to give the full-sandwich germacarborane and an additional equivalent of $SnCl_2$.[30] In the absence of excess stannacarborane, the half-sandwich germacarborane results.

The results outlined in Scheme 1 are consistent with those found for the solvent-mediated reactions of $GeCl_4$ with the group 1 compounds of the carboranes.[7,9a] It has been shown that the reaction of the monolithium compound $Li^+[2,3\text{-}(SiMe_3)_2\text{-}2,3\text{-}C_2B_4H_5]^-$ with $GeCl_4$ in a 2:1 molar ratio in THF solvent, at 0 °C, produced the corresponding *commo*-germacarborane in 10% yield and the *closo*-germacarborane in 14% yield, as well as substantial amounts of the neutral carborane (48% yield).[9a] Similarly, the reaction of the mixed Na/Li compounds of the $[2\text{-}(SiMe_3)\text{-}3\text{-}(R)\text{-}2,3\text{-}C_2B_4H_4]^{2-}$ (R = $SiMe_3$, Me, and H) dianions with $GeCl_4$ in 2:1 carborane-to-germanium molar ratios in THF at 0 °C afforded similar mixtures of the full- and half-sandwich germacarboranes, as well as the neutral carboranes.[7] For comparison, when R = $SiMe_3$, the yields in these reactions were 18%, 36%, and 33%, respectively (based on the carborane consumed), which accounted for 87% of the initial carborane. The product distributions when R = Me and H were similar, but the overall yields were lower.[7] Significantly, there was no evidence for the formation of Ge(IV)-substituted germacarboranes, such as **IV**−**VI**; these are produced only in the absence of solvent and with excess $GeCl_4$, as described in the Experimental Section.

There are two Lewis-acid sites in **IV**−**VI**, the apical Ge(II) and the exopolyhedral Ge(IV). While one might expect that the higher oxidation state germanium would be the site for base coordination, just the opposite was found experimentally. With the possible exception of the reaction with the (ferrocenylmethyl)-*N*,*N*-dimethylamine (ferrocene amine) base, all Lewis bases studied (2,2′-bipyridine ($C_{10}H_8N_2$), 2,2′-bipyrimidine ($C_8H_6N_4$), and 2,2′:6′:2″-terpyridine ($C_{15}H_{11}N_3$)) bond exclusively to the apical Ge(II) rather than to the Ge(IV) site. The yields of the acid−base reactions range from 40% for the reaction of **IV** with $C_8H_6N_4$ to 67% for the reaction of the same germacarborane with $C_{15}H_{11}N_3$. The unsubstituted bipyridine−germacarborane complexes 1-Ge-($C_{10}H_8N_2$)-2-($SiMe_3$)-3-(R)-2,3-$C_2B_4H_4$ have been synthesized by the reaction of the corresponding *closo*-germacarborane with $C_{10}H_8N_2$ in yields of 73% for R = $SiMe_3$ and 42% for R = Me,[7] which are similar to those found for compounds **VII** and **VIII** (63% and 59%, respectively). It is of interest to note that the reaction of the unsubstituted germacarboranes with the bis(bidentate) ligand $C_8H_6N_4$ resulted in only 1:1 donor−acceptor complexes[14a] rather than the bridged compounds **IX** and **X** and the corresponding bipyrimidine−stannacarborane complexes.[15b]

The products found in the reaction of **IV** with the strong monodentate base, ferrocene amine, are quite different from those obtained when the metallacarborane reacts with the bidentate bases (see above) or when the ferrocene amine reacts with the unsubstituted germacarborane, 1-Ge-2,3-$(SiMe_3)_2$-2,3-$C_2B_4H_4$.[14b] Instead of a simple acid−base adduct formation, the reaction of **IV** with ferrocene amine produces a 1:1 mixture of the salt $\{[(\eta^5\text{-}C_5H_5)Fe(\eta^5\text{-}C_5H_4CH_2]_2N(Me)_2\}^+$-$\{GeCl_3\}^-$ (**XII**) and **XIII**, which is a ferrocene amine−

Scheme 2

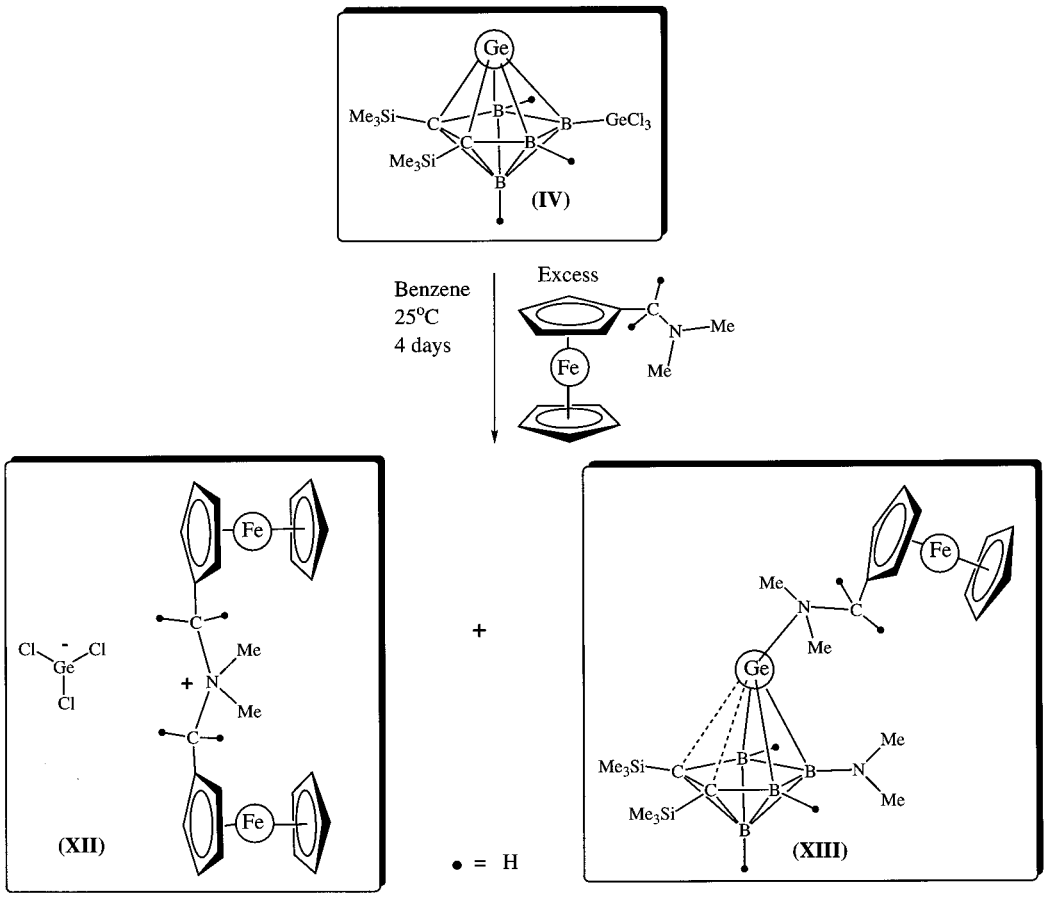

germacarborane complex in which an $N(Me)_2$ group has replaced the exopolyhedrally bound $GeCl_3$ (see Scheme 2). As can be seen from Scheme 2, the reaction involves an oxidative coupling of two ferrocene amines, the formation of a trichlorogermanate(II) ion, and a new β-amino−germacarborane complex (**XIII**). These products are the results of a sequence of reactions that involve, at least formally, nucleophillic attacks on the capping Ge(II), the unique boron of the $GeCl_3$-substituted germacarborane, and the methylene carbon of a ferrocene amine fragment. Although neither the sequence of reactions nor their mechanisms are known, it is clear that none of the products would be the result of attack on the Ge(IV) center.

Even though two germanium atoms are present in **IV**−**VI**, no evidence has been found to indicate that the Ge(IV) atoms in these compounds act as Lewis-acid sites. An inspection of the LUMO and LUMO + 1 molecular orbitals obtained from ab initio calculations at the HF/3-21G* level of theory on the model compound 5-$GeCl_3$-1,2,3-$GeC_2B_4H_5$ shows localization only on the apical Ge(II) and carborane cage. Therefore, from frontier orbital considerations, one would predict that the lower valence apical germanium would be the preferred reaction site for a nucleophile, which is what is found experimentally.

Crystal Structures of *closo*-1-Ge-2-($SiMe_3$)-3-(R)-5-($GeCl_3$)-2,3-$C_2B_4H_3$ (R = $SiMe_3$ (IV), Me (V), and H (VI)), 1-Ge($C_{10}H_8N_2$)-2,3-($SiMe_3$)$_2$-5-($GeCl_3$)-2,3-$C_2B_4H_3$ (VII), 1,1′-(2,2′-$C_8H_6N_4$)-[1-Ge-2,3-($SiMe_3$)$_2$-5-($GeCl_3$)-2,3-$C_2B_4H_3$]$_2$ (IX), and {[(η^5-C_5H_5)Fe(η^5-$C_5H_4CH_2$]$_2$N(Me)$_2$}$^+$[$GeCl_3$]$^-$ (XII). The solid-state structures of **IV**−**VII**, **IX**, and **XII**, as determined by single-crystal X-ray diffraction, are shown in Figures 1−6, respectively. Table 4 lists some important bond distances and bond angles.

The structures of compounds **IV**, **V**, and **VI** show them to be digermanium complexes in which a Ge, in a formal +2 state, occupies the apical position above the planar, pentagonal C_2B_3 face of the carborane ligand, with the second germanium, in a formal +4 state, being involved in an exopolyhedral $GeCl_3$ group bonded to the unique boron of the cage. The distances listed in Table 4 show that the carborane ligands are η^5-bonded to the capping germanium atoms, with the average Ge−C_2B_3 atom distances being 2.251 ± 0.006 Å in **IV**, 2.266 ± 0.013 Å in **V**, and 2.262 ± 0.009 Å in **VI**.[31] These distances are similar to the average Ge−C_2B_3 distances of 2.228 ± 0.021 Å found in *closo*-1-Ge-2,4-($SiMe_3$)$_2$-2,4-$C_2B_4H_4$ and 2.23 ± 0.13 Å found in *commo*-1,1′-Ge(2,3-($SiMe_3$)$_2$-1,2,3-$GeC_2B_4H_4$)$_2$[6,9a,30] but are significantly shorter than the average Ge−C_5 distance of 2.517 ± 0.131 Å found in germanocene.[32] However, the structures of **IV**−**VI** differ from those of germanocene and the *commo*-germacarborane in that the germanium atoms in the latter two complexes are not symmetrically bonded to their respective ligands but are displaced or slipped off of the centroidal positions. Slippage in the germanocene is such that the Ge−C distances range from 2.347 to 2.730 Å,[32] while in the *commo*-germacar-

(31) Whenever an average value of a parameter is given, the listed indetermination is the average deviation.

(32) Grenz, M.; Hahn, E.; du Mont, W. W.; Pickart, J. *Angew. Chem.* **1985**, *96*, 68.

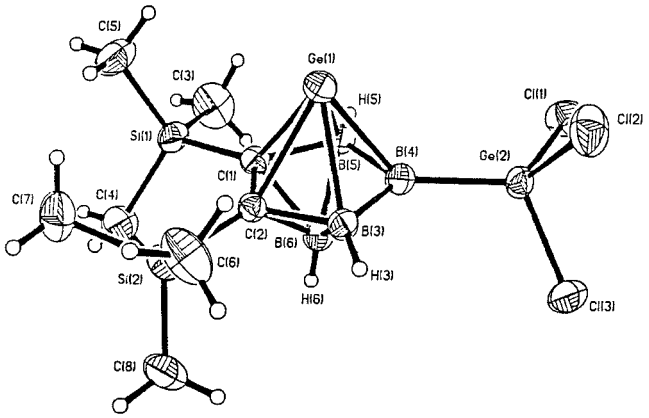

Figure 1. Perspective view of *closo*-1-Ge-2,3-$(SiMe_3)_2$-5-$(GeCl_3)$-2,3-$C_2B_4H_3$ (**IV**), showing the atom-numbering scheme. Thermal ellipsoids are drawn at the 40% probability level.

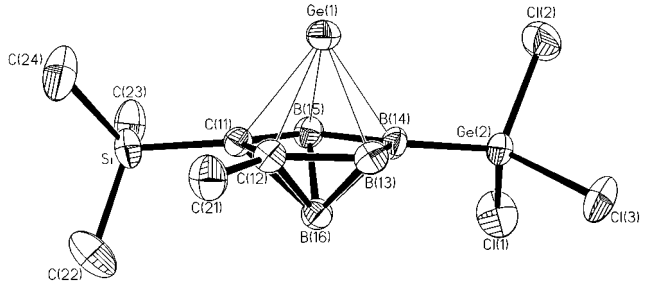

Figure 2. Perspective view of *closo*-1-Ge-2-$(SiMe_3)$-3-(Me)-5-$(GeCl_3)$-2,3-$C_2B_4H_3$ (**V**), showing the atom-numbering scheme. Thermal ellipsoids are drawn at the 40% probability level.

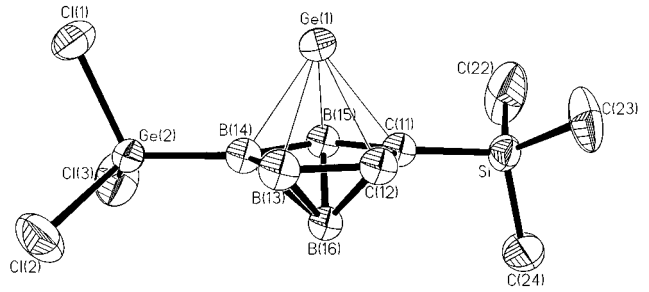

Figure 3. Perspective view of *closo*-1-Ge-2-$(SiMe_3)$-3-(H)-5-$(GeCl_3)$-2,3-$C_2B_4H_3$ (**VI**), showing the atom-numbering scheme. Thermal ellipsoids are drawn at the 40% probability level.

borane the distances vary from 2.08 Å for the unique boron (equivalent of B(4) in Figure 1) to 2.38 and 2.39 Å for the two cage carbons.[9a,30] Inspection of the individual Ge−C_2B_3 atom distances for compounds **IV**−**VI**, given in Table 4, reveals no systematic variation consistent with a slip distortion. The lack of metal slippage in **IV**, compared with the *commo*-germacarborane and other main-group metallacarboranes, was rationalized on the basis that replacement of the terminal hydrogen on the unique boron with the more electronegative $GeCl_3$ group should decrease electron density around the boron atom, thereby attenuating bonding between this atom and the capping metal. Such a weakened interaction would tend to diminish slippage of the metal toward the boron atoms.[8] Unfortunately, even though the unsubstituted *closo*-germacarboranes *closo*-1-Ge-2-$(SiMe_3)$-3-(R)-2,3-$C_2B_4H_4$ (R = $SiMe_3$, Me, H) have been prepared and characterized, their structures could not be measured.[7] Therefore, a direct assessment of the structural effect of a H/$GeCl_3$ substitution is not possible. However, the geometries of the model compounds *closo*-1,2,3-$GeC_2B_4H_6$ (**XIV**) and 5-$GeCl_3$-1,2,3-$GeC_2B_4H_5$ (**XV**) optimized at the B3LYP/6-31G* level of theory give structures with very similar Ge−C_2B_3 atom distances; using the atom-numbering system in Figure 1, the relevant distances in **XIV** and **XV** (given in parentheses) are Ge−C(1,2) = 2.281 Å (2.327 Å); Ge−B(3,5) = 2.243 Å (2.254 Å); Ge−B(4) = 2.184 Å (2.153 Å). Since little variation was found in the theoretical distances, it would be expected that any structural effects of a $GeCl_3$ substitution would probably be small and could be lost in the experimental indeterminations.

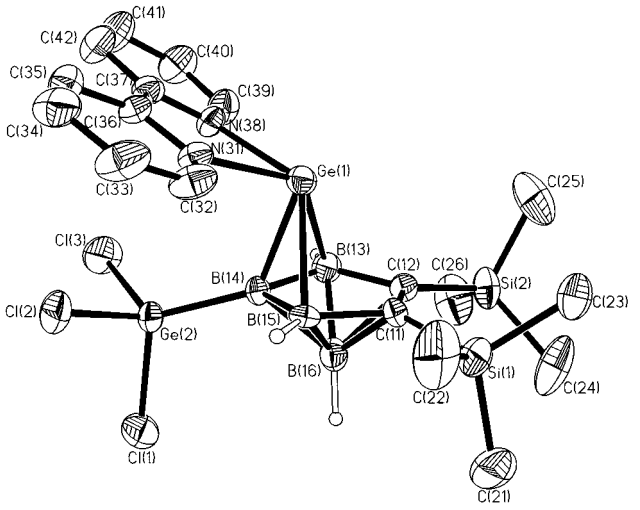

Figure 4. Perspective view of 1-Ge(2,2′-$C_{10}H_8N_2$)-2,3-$(SiMe_3)_2$-5-$(GeCl_3)$-2,3-$C_2B_4H_3$ (**VII**), showing the atom-numbering scheme. Thermal ellipsoids are drawn at the 40% probability level. For clarity, all H's except the carborane cage are removed.

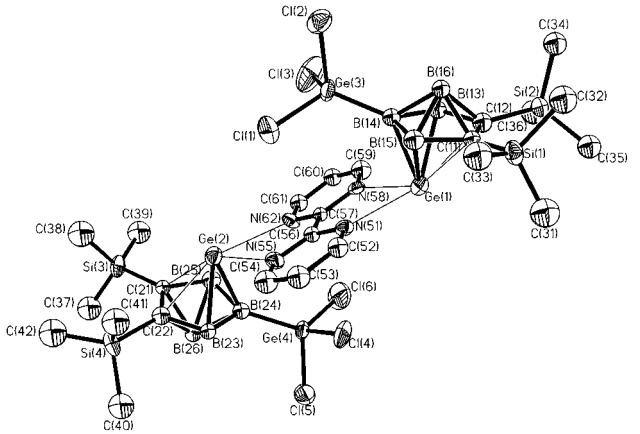

Figure 5. Perspective view of "bridged" donor−acceptor complex 1,1′-(2,2′-$C_8H_6N_4$)-[1-Ge-2,3-$(SiMe_3)_2$-5-$(GeCl_3)$-2,3-$C_2B_4H_3]_2$ (**IX**), showing the atom-numbering scheme. Thermal ellipsoids are drawn at the 40% probability level. For clarity, all H's are removed.

Figures 4 and 5 show that coordination of the capping germanium by either 2,2′-$C_{10}H_8N_2$ (**VII**) or 2,2′-$C_8H_6N_4$ (**IX**) disrupts the η^5-bonding posture of the carboranes, leading to significantly distorted complexes. The Ge(II)−C_2B_3 bond distances in **VII** are Ge−C(11) = 2.761(6) Å; Ge−C(12) = 2.806(6) Å; Ge−B(13) = 2.443(7) Å;

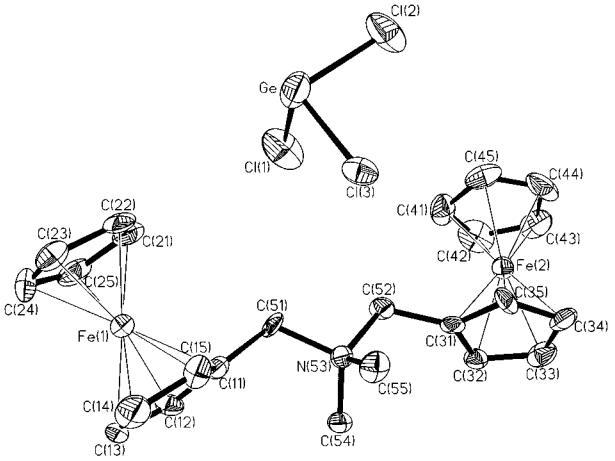

Figure 6. Perspective view of $\{[(\eta^5\text{-}C_5H_5)Fe(\eta^5\text{-}C_5H_4\text{-}CH_2)]_2N(Me)_2\}^+[GeCl_3]^-$ (**XII**), showing the atom-numbering scheme. Thermal ellipsoids are drawn at the 40% probability level. For clarity, methyl and methylene H's are not shown.

Ge−B(15) = 2.407(7) Å; Ge−B(14) = 2.173(7) Å and in **IX** are Ge(1,2)−C(11,21) = 2.577, 2.455 Å; Ge(1,2)−C(12,22) = 2.565, 2.443 Å; Ge(1,2)−B(13,23) = 2.337, 2.284 Å; Ge(1,2)−B(15,25) = 2.308, 2.303 Å; Ge(1,2)−B(14,24) = 2.193, 2.200 Å. A comparison of these distances with the analogous Ge−C_2B_3 distances in **IV** shows that the Ge−C(cage) distances increase by ∼0.5 Å in **VII** and ∼0.3 Å in **IX**, the Ge−B(basal) distances increase by ∼0.2 and ∼0.05 Å, while the Ge−B(unique) distances decrease slightly on complexation, by ∼0.07 Å in **VII** and ∼0.05 Å in **IX**. On the other hand, the Ge(IV)−B(unique) distance seem unaffected by complexation. The slippages of the capping germaniums are such that the carboranes are better described as being η^3- bonded to the metals. Slip distortions such as these are common facets of the group 13 and group 14 metallacarborane coordination chemistry[6] and have been explained by noting that complexation of the capping metal by a base preferentially weakens the metal−cage bonds opposite the base, which, in the case of the carbons adjacent complexes are the cage carbons. Slippage also relieves electron−electron repulsion between the base and the carborane ligands, thereby allowing stronger base−metal bonding.[33] These same factors are most likely responsible for the slip distortions found in compounds **VII** and **IX**. The structures of both the bipyridine[7] and the bipyrimidine[14a] complexes of the unsubstituted germacarborane *closo*-1-Ge-2,3-$(SiMe_3)_2$-2,3-$C_2B_4H_4$ have been determined so that direct comparisons with **VII** and **IX** are possible. In the unsubstituted germacarborane−bipyridine complex, the two nitrogens of the base were not symmetrically bonded to the capping germanium, the distances being 2.321(4) and 2.474(4) Å, which are significantly longer than the analogous distances of 2.215 ± 0.010 Å in **VII**, given in Table 4. The shorter metal−base bond distances are consistent with an increase in the Lewis acidity of the capping metal on substitution of the terminal hydrogen of the unique boron with a $GeCl_3$ group. A stronger metal−base bonding in **VII** is also reflected in a larger slip distortion; using the numbering system given in Figure 4, the Ge−C_2B_3 distances in the unsubstituted complex are Ge−C(11,12) = 2.579(5), 2.510(5) Å; Ge−B(13,15) = 2.255(7), 2.371(7) Å; Ge−B(14) = 2.208(7) Å.[7] A comparison of these values with the analogous Ge−C_2B_3 distances in **VII** shows shorter Ge−C distances and a longer Ge−B(unique) distance in the unsubstituted base−germacarborane complex, indicative of a smaller slip distortion. The Ge−carborane bond distances in the unsubstituted germacarborane−bipyrimidine complex were found to be Ge−C(11) = 2.539(12) Å; Ge−C(12) = 2.528(12) Å; Ge−B(13) = 2.269(17) Å; Ge−B(15) = 2.330(16) Å; Ge−B(14) = 2.189(15) Å,[14a] which are comparable to the shorter set of distances found for **IX**, as listed in Table 4. However, in the case of unsubstituted germacarborane, the bipyrimidine functions only as a bidentate base, rather than as a bis(bidentate) ligand, so the equivalent bond distances found in the two complexes are consistent with $GeCl_3$ substitution enhancing the Lewis acidity of the capping germanium atom.

The only non-carborane whose structure is given in this report is that of the salt, $\{[(\eta^5\text{-}C_5H_5)Fe(\eta^5\text{-}C_5H_4\text{-}CH_2)]_2N(Me)_2\}^+[GeCl_3]^-$ (**XII**), which is shown in Figure 6. Figure 6 provides structural information on an isolated trichlorogermanate(II) ion. Although this ion was first isolated in the 1930s as its cesium salt, $CsGeCl_3$[34] and the reactions of the anion with both organic[35] and inorganic[35] compounds have been reported, little is known about its structure. The far-infrared studies of several salts and adducts of $[GeCl_3]^-$ indicated C_{3v} symmetry.[36a,37] Room-temperature single-crystal X-ray diffraction studies of $CsGeCl_3$ show that the compound is dimorphic, crystallizing at room temperature in a distorted perovskite structure in which three short (2.31 Å) and three long (3.13 Å) Ge−Cl distances were found, with a higher temperature (>155 °C) cubic form having six equivalent Ge−Cl distances of 2.74 Å, which is close to the average of the two distances found at room temperature.[38] In contrast, the crystal packing diagram of **XII**, given in Figure 7, shows that the trichlorogermanate(II) ions are well-separated in the unit cell, so that the structure shown in Figure 6 is a good approximation to that of an "isolated" $[GeCl_3]^-$ anion. The anion in **XII** has the expected C_{3v} symmetry with three equal Ge−Cl bonds at distances of 2.281 ± 0.004 Å and angles of 95.3 ± 0.7° (see Table 4). These bond distances are shorter than those in $CsGeCl_3$ but longer than the Ge−Cl distances found in compounds **IV**−**VI**, which are 2.145 ± 0.006, 2.130 ± 0.001, and 2.148 ± 0.004 Å, respectively. In addition to shorter bond distances, the Cl−Ge−Cl bond angles in the $GeCl_3$-substituted germacarboranes average ∼104°, which is significantly greater than those found in **XII** (see Table

(33) (a) Barreto, R. D.; Fehlner, T. P.; Hosmane, N. S. *Inorg. Chem.* **1988**, *27*, 453. (b) Maguire, J. A.; Ford, G. P.; Hosmane, N. S. *Inorg. Chem.* **1988**, *27*, 3354. (c) Maguire, J. A.; Fagner, J. S.; Siriwardane, U.; Banewicz, J. J.; Hosmane, N. S. *Struct. Chem.* **1990**, *1*, 583. (d) Hosmane, N. S.; Zhang, H.; Lu, K.-J.; Maguire, J. A.; Cowley, A. H.; Mardones, M. A. *Struct. Chem.* **1992**, *3*, 183.

(34) Karantaesis, T.; Capatos, L. *Compt. Rend.* **1935**, *201*, 74.

(35) (a) Poskozim, P. S. *J. Organomet. Chem.* **1968**, *12*, 115. (b) Poskozim, P. S.; Stone, A. L. *J. Organomet. Chem.* **1969**, *16*, 314.

(36) (a) Johnson, M. D.; Shriver, D. F.; Shriver, S. A. *J. Am. Chem. Soc.* **1966**, *88*, 1588. (b) Jutzi, P.; Hampel, B. *J. Organomet. Chem.* **1986**, *301*, 283.

(37) Poskozim, P. S.; Stone, A. L. *J. Inorg. Nucl. Chem.* **1970**, *32*, 1391.

(38) (a) Christensen, A. N.; Rasmussen, S. E. *Acta Chem. Scand.* **1965**, *19*, 421. (b) Thiele, G.; Rotter, H. W.; Schmidt, K. D. *Z. Anorg. Allg. Chem.* **1987**, *545*, 148.

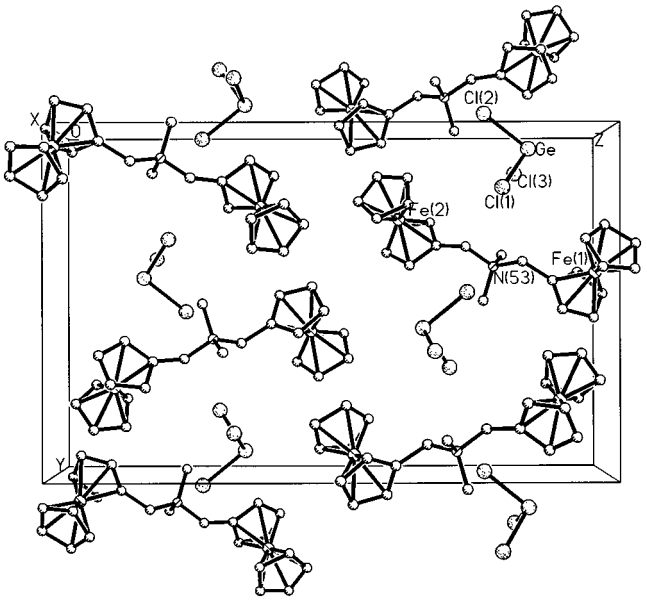

Figure 7. Crystal packing diagram of $\{[(\eta^5\text{-}C_5H_5)Fe(\eta^5\text{-}C_5H_4CH_2)]_2N(Me)_2\}^+[GeCl_3]^-$ (**XII**).

4). An increase in bond angles and a decrease in bond distances would be expected when $[GeCl_3]^-$ coordinates.

Spectra. The IR spectra of compounds **IV**−**XI** and **XIII** (Table 2) all show absorptions around 2600 cm^{-1} due to BH stretching mode of vibrations. The IR absorptions due to C═N stretching vibrations in 2,2′-bipyridine, 2,2′-bipyrimidine, and 2,2′:6′,2″-terpyridine are also present near 2280, 2284, and 3098 cm^{-1}, respectively. These observations are all consistent with the formula proposed for **IV**−**XI** and **XIII** but offer little insight into the various bonding interactions that contribute to the structures of these compounds. Unfortunately, the range of the spectrophotometers available to us did not permit an investigation of the far-infrared region where the Ge−Cl stretches are normally found.

All compounds were characterized by their ^1H, ^{13}C, and ^{11}B NMR spectra; the results are summarized in Table 2. All spectra show the appropriate resonances for the various groups present with the expected relative peak areas and are consistent with the structures proposed and with those shown in Figures 1−6. The ^{11}B NMR spectra of **IV**−**VI**, which are expected to be most sensitive to the nature of the capping metal group, all show an upfield resonance at δ −4.60 (**IV**), −3.45 (**V**), and −5.09 ppm (**VI**), due to the apical borons, with the resonances of the less-shielded facial borons being shifted downfield by 24−28 ppm (see Table 1). Table 1 also shows that coordination of the apical germanium by either the $C_{10}H_8N_2$ or $C_8H_6N_4$ base generally leads to upfield shifts of the apical boron resonances from 11.13 (for **X**) to 23.45 ppm (for **VII**), with the facial boron shifts being much lower (∼3−10 ppm). On the other hand, the chemical shifts in **XI**, which is the terpyridine complex of **IV**, undergo much smaller changes than those found for the other two base−germacarborane complexes, with the apical boron resonance being shifted upfield from **IV** by 5.78 ppm while the facial borons are slightly deshielded and show a downfield shift of 2.68 ppm. The ^{11}B NMR chemical shifts of the group 14 metallacarboranes have been qualitatively rationalized by noting that, at least formally, the capping metal competes with the apical boron for electron density of the C_2B_3 face. Therefore, any interaction that increases metal−carborane bonding should withdraw electron density from the apical boron, with the facial atoms being less affected.[33b,c] These arguments help rationalize the changes in the ^{11}B NMR spectra seen in the syntheses and reactions of the germacarboranes. When the metal first bonds to the carborane ligand, there is a large downfield shift of the apical boron resonances from the δ −40 to −50 ppm range in the dianions to the δ 0 to −5 ppm range found in **IV**−**VI**. Coordination of the capping metal with a base would tend to decrease metal−carborane bonding and restore, at least to some extent, electron density back on the apical boron, which should result in a shift back upfield. This general pattern is found in the present work. However, it has been shown that factors other than gross electron density are also important in determining the shielding of the cage boron atoms in heterocarboranes.[40] Since the unsubstituted germacarborane analogues of **IV**−**X** have been prepared and their ^{11}B NMR spectra determined, the effects of $GeCl_3$ substitution on the NMR spectra can be assessed. Table 5 lists the ^{11}B NMR

Table 5. ^{11}B NMR Chemical Shifts of Some Germacarboranes

compd	δ, ppm[a] (rel. area)	ref or method
2,3-$(SiMe_3)_2$-1,2,3-$GeC_2B_4H_4$	24.1(3), −1.5(1)	7
2-$SiMe_3$-3-Me-1,2,3-$GeC_2B_4H_4$	20.5(3), −0.0(1)	7
	21.9(1), 21.8(1), 20.9(1), −0.3(1)	GIAO[b,c]
2-$SiMe_3$-1,2,3-$GeC_2B_4H_5$	14.2(1), 10.1(2), −0.1(1)	7
	23.6(1), 20.5(1), 18.5(1), −2.4(1)	GIAO[b,d]
1-(FA)-2,3-$(SiMe_3)_2$-1,2,3-$GeC_2B_4H_4$[e]	18.85(3), −7.83(1)	14b
1-$(C_{10}H_8N_2)$-2,3-$(SiMe)_2$-1,2,3-$GeC_2B_4H_4$	23.1(3), −5.3(1)	39
1-$(C_8H_6N_4)$-2,3-$(SiMe_3)_2$-1,2,3-$GeC_2B_4H_4$	23.5(3), −4.3(1)	14a
	27.2(1), 23.7(2), −5.0(1)	GIAO[f]
1,2,3-$GeC_2B_4H_6$ (XIV)	21.6(1), 16.6(2), −3.2(1)	GIAO[b]
5-$GeCl_3$-1,2,3-$GeC_2B_4H_5$ (XV)	20.1(1), 17.0(2), −5.7(1)	GIAO[b]
1-NH_3-5-NH_2-1,2,3$GeC_2B_4H_5$	42.52(1), 3.48(2), −14.84(1)	GIAO[b]
1-NH_3-5-$GeCl_3$-1,2,3-$GeC_2B_4H_5$	21.70(1), 11.43(2), −12.92(1)	GIAO[b]
1-NH_3-1,2,3-$GeC_2B_4H_6$	29.91(1), 8.51(2), −13.77(1)	GIAO[b]
1-NH_3-4-NH_2-1,2,3-$GeC_2B_4H_5$	19.36(1), 19.29(1), 0.90(1), −11.29(1)	GIAO[b,g]

[a] Relative to $BF_3{\cdot}(C_2H_5)_2O$. [b] At the HF/6-311G** level on B3LYP/6/31G* optimized geometries. [c] The shielding order is B(15) < B(13) < B(14) < B(16) as defined in Figure 2. [d] The shielding order is B(14) < B(15) < B(13) < B(16) as defined in Figure 3. [e] FA = (ferrocenylmethyl)-*N*,*N*-dimethylamine, $[(\eta^5\text{-}C_5H_5)Fe(\eta^5\text{-}C_5H_4CH_2(Me)_2N)]$. [f] At the HF/6-311G** level on a HF/6-311G** optimized geometry. [g] The shielding order is B(5)(NH_2) > B(4) > B(3) > B(6) as defined in Figure 1.

(39) Hosmane, N. S.; Siriwardane, U.; Islam, M. S.; Maguire, J. A.; Chu, S. S. C. *Inorg. Chem.* **1987**, *26*, 3428.

(40) (a) Hermánek, S.; Hnyk, D.; Havlas, Z. *J. Chem. Soc., Chem. Commun.* **1989**, 1859. (b) Bühl, M.; Schleyer, P. v. R.; Havlas, Z.; Hnyk, D.; Hermánek, S. *Inorg. Chem.* **1991**, *30*, 3107. (c) Fehlner, T. P.; Czech, P. T.; Fenske, R. F. *Inorg. Chem.* **1990**, *29*, 3103.

chemical shifts found or calculated for a number of unsubstituted germacarboranes. A comparison of the chemical shifts in ^{11}B NMR spectra of **IV**−**VI**, listed in Table 1, with their respective unsubstituted germacarboranes, given in Table 5, shows that, with the exception of the mono(trimethylsilyl)germacarboranes [1-Ge-2-($SiMe_3$)-3-(R)-2,3-$C_2B_4H_5$, (R = $GeCl_3$ (**IV**) or H), very little change is found. The ^{11}B NMR spectra of both sets of compounds show two resonances, one in the δ 20 to 25 ppm range due to the facial borons, with the apical boron resonances being shifted upfield by 21−28 ppm. It is of interest to note that substitution of a $GeCl_3$ for a H on the unique boron does not affect the chemical shift of that atom to any measurable extent; δ = 23.59 ppm for **IV** and 20.13 ppm in **V**, compared to 24.1 and 20.5 ppm for their respective unsubstituted analogues.[7] The largest changes are found in the apical boron resonances, which shift upfield by ∼3 ppm on $GeCl_3$ substitution (see Tables 1 and 5). A similar insensitivity to the nature of the substituent on the unique boron is also seen in the ^{13}C NMR chemical shifts, where the substituted and unsubstituted forms of **IV** and **V** are the same to within 1−2 ppm.[7] However, while the spectra of **IV** and **V** are very similar to those of their unsubstituted analogues and to those calculated for the model compound **XV**, the same is not true for compound **VI**. Table 5 lists the ^{11}B NMR chemical shifts for 2-($SiMe_3$)-1,2,3-$GeC_2B_4H_5$,[7] which differ significantly from those listed in Table 1, as well as its GIAO-calculated values. At present, there is no ready explanation for this discrepancy.

The structure of compound **XIII** was assigned on the basis of chemical analysis and its ^{1}H, ^{11}B, and ^{13}C NMR and IR spectra. The ^{1}H NMR spectrum shows two resonances at δ 1.98 and 1.76 ppm whose peak areas and general locations are consistent with NMe_2 protons. Two NMe_2 resonances, at δ 43.70 and 39.35 ppm, were also found in the ^{13}C NMR spectrum of **XIII** (see Table 1). The ^{11}B NMR spectrum of the compound showed a broad envelope of resonances with peaks at δ 36.75, 8.6, 6.8, and −11.78 ppm in a roughly 1:1:1:1 peak area ratio. Only the resonances at δ 36.75 and −11.78 ppm were separated enough that the δ's have significance. Since the unique and basal boron resonances could not be resolved, it was not possible to verify the location of the NMe_2 group from the absence of B−H coupling. The ^{11}B NMR spectra of the ferrocene amine complex of the unsubstituted germacarborane 1-[(η^5-C_5H_5)Fe(η^5-C_5H_4-$CH_2(Me)_2N$)]-2,3-($SiMe_3$)$_2$-1,2,3-$GeC_2B_4H_4$[14b] shows two resonances at δ 18.85 and −7.83 ppm, with a 3:1 peak area ratio (see Table 5). The rather large downfield shift of ∼14 ppm of one of the facial boron resonances found in going from the unsubstituted complex to **XIII** is consistent with the reasonable assumption that the presence of the more electronegative NMe_2 on the boron would significantly deshield it and cause a large downfield shift of its resonance. It is of interest to note that the apical boron resonances are much less affected by such a substitution; the apical resonances of the two ferrocene amine complexes differ by only 4 ppm. It should be pointed out that the assumption that the NMe_2 group bonds to the unique boron is made on the basis of the known structure of its precursor **IV**; there is no direct spectral evidence that would preclude substitution on one of the basal borons; indeed, the peak area ratios are consistent with such a substitution.

Conclusions

Our studies have shown that substitution of the terminal hydrogen on the unique boron of half-sandwich germacarboranes by a $GeCl_3$ group does not materially affect either the geometry, spectral properties, or general reactivity patterns of the metallacarborane. The major effect is that $GeCl_3$ substitution enhances the Lewis acidity of the capping germanium, presumably by withdrawing some electron density from the cage. All evidence indicates that this withdrawal is mainly from the capping metal and the apical boron. No evidence was found for the Ge(IV) atoms being the centers for reactivity.

Acknowledgment. This work was supported by grants from the Robert A. Welch Foundation (Grant Nos. N-1016 and N-1322), the donors of the Petroleum Research Fund, administered by the American Chemical Society, and the National Science Foundation.

Supporting Information Available: Tables of atomic coordinates (Table S-1), selected bond lengths and angles (Table S-2), anisotropic displacement parameters (Table S-3), H-atom coordinates, and isotropic displacement coefficients (Table S-4) for **IV**, **V**, **VI**, **VII**, **IX**, and **XII** (30 pages). Ordering information is given on any current masthead page.

OM980183M